Published April 29, 2002

Openings of the Rat Recombinant α1 Homomeric Glycine Receptor as a Function of the Number of Agonist Molecules Bound

Marco Beato,[1] Paul J. Groot-Kormelink,[1] David Colquhoun,[2] and Lucia G. Sivilotti[1]

[1]Department of Pharmacology, The School of Pharmacy, London WC1N 1AX, United Kingdom
[2]Department of Pharmacology, University College London, London WC1E 6BT, United Kingdom

ABSTRACT The functional properties of rat homomeric α1 glycine receptors were investigated using whole-cell and outside-out recording from human embryonic kidney cells transfected with rat α1 subunit cDNA. Whole-cell dose-response curves gave EC_{50} estimates between 30 and 120 μM and a Hill slope of ~3.3. Single channel recordings were obtained by steady-state application of glycine (0.3, 1, or 10 μM) to outside-out patches. Single channel conductances were mostly 60–90 pS, but smaller conductances of ~40 pS were also seen (10% of the events) with a relative frequency that did not depend on agonist concentration. The time constants of the apparent open time distributions did not vary with agonist concentration, but short events were more frequent at low glycine concentrations. There was also evidence of a previously missed short-lived open state that was more common at lower glycine concentrations. The time constants for the different components of the burst length distributions were found to have similar values at different concentrations. Nevertheless, the mean burst length increased with increasing glycine. This was because the relative area of each burst-length component was concentration dependent and short bursts were favored at lower glycine concentrations. Durations of adjacent open and shut times were found to be strongly (negatively) correlated. Additionally, long bursts were made up of longer than average openings separated by short gaps, whereas short bursts usually consisted of single isolated short openings. The most plausible explanation for these findings is that long bursts are generated when a higher proportion of the five potential agonist binding sites on the receptor is occupied by glycine. On the basis of the concentration dependence and the intraburst structure we provide a preliminary kinetic scheme for the activation of the homomeric glycine receptor, in which any number of glycine molecules from one to five can open the channel, although not with equal efficiency.

KEY WORDS: single channel • patch clamp • HEK • recombinant receptors • homomeric receptors

INTRODUCTION

Glycine is the main inhibitory neurotransmitter in the spinal cord and in the brainstem. The first description of its inhibitory effects was given by Werman et al. (1967), who showed that iontophoretically-applied glycine inhibited firing in spinal motoneurones. Since then, glycine receptors (GlyRs)* have been found not only in the spinal cord, but also in most areas of the brainstem in retinal ganglion cells and in the olfactory bulb (Legendre, 2001).

GlyRs have a pentameric structure consisting of a central ion channel surrounded by five subunits, which have four transmembrane domains and thus belong to the nicotinic superfamily. Up to now, five subunits (four α and one β) have been cloned, far fewer than for $GABA_A$ or neuronal nicotinic receptors. Only the α subunits can form functional homomeric channels when expressed in heterologous expression systems. Such homomeric GlyRs are important in the developing nervous system, but may be replaced by α/β heteromers in the adult (for review see Kuhse et al., 1995; Legendre, 2001). There have been many investigations of the stoichiometry of heteromeric GlyR, the domains in the sequence that determine specific assembly, and the mechanism of GlyR clustering by associated proteins such as gephyrin and collybistin (see Kuhse et al., 1995; Kins et al., 2000).

Biophysical investigations on GlyRs focused initially on the different single-channel conductance levels observed with the expression of different subunits, on the anion permeability of GlyRs, and on the identification of the amino acid residues responsible for these properties (Bormann et al., 1987, 1993; Keramidas et al., 2000). Another line of investigation arose from the discovery that both a human congenital neurological disease, hyperekplexia or startle disease, and some inherited neurological syndromes in mice (*spastic*, *spasmodic* and *oscillator*) are caused by mutations in GlyR subunits (mostly on the α1 subunit). Several such mutations in human GlyRs have now been identified and characterized by expression in heterologous systems. Although

Address correspondence to Marco Beato at his current address: Department of Pharmacology, University College London, Gower St., London WC1E 6BT. Tel.: (44) 20-7679 3765; Fax (44) 20-7679 7298; E-mail m.beato@ucl.ac.uk

*Abbreviations used in this paper: EGFP, enhanced green fluorescent protein; GlyR, glycine receptor.

Published April 29, 2002

only a minority of these mutations affect the relative abundance of single-channel conductance levels, all reduce GlyR sensitivity to agonists (Legendre, 2001). This effect has been attributed to impairment either in the affinity of glycine binding (Langosch et al., 1994), or in the probability that the channel will open once it has bound glycine (Rajendra et al., 1994). Much of the uncertainty in deciding between these two possibilities stems from the lack of an established mechanism for the activation of mammalian GlyR. Some insight can be gained by assuming the simplest plausible activation mechanism for GlyRs (Lewis et al., 1998; see also the investigation of the effects of zinc ions by Laube et al. [2000]). Nevertheless, this approach is less than satisfactory, especially since we already know that this simplest mechanism (several binding steps followed by isomerization to one open state) is wrong. This follows from the first single-channel kinetic study on GlyR (Twyman and Macdonald, 1991), which showed clearly that these receptors have at least three distinguishable open states. Another important feature of this work was the observation that the distributions of burst durations are concentration-dependent (Twyman and Macdonald, 1991). This phenomenon (confirmed by Fucile et al. [1999] in zebrafish α1 recombinant GlyRs) poses important constraints to the type of mechanism that can describe the activation of GlyRs. The most obvious explanation is that GlyRs can open with different kinetics at different levels of ligation, in a manner similar to the muscle nicotinic receptor.

The aim of the present work is to extend the available evidence on the kinetic behavior of recombinant GlyRs of known subunit composition (i.e., rat homomeric α1 GlyR expressed in HEK293 cells). In particular, we provide a detailed analysis of intraburst structure at a range of agonist concentrations for these receptors, in order to test the hypothesis that openings can occur when not all the glycine binding sites are occupied. We also discuss the implications of these new data for GlyR activation schemes that are physically plausible for a homomeric pentamer such as the α1 GlyR. It is only by establishing a physically correct mechanism of GlyR activation that we shall be able to interpret the effects of mutations and hence understand the function of the different domains in the receptor's sequence. This question is also of physiological relevance, because answering it is important to our understanding of glycinergic synaptic transmission and how it is affected by GlyR mutations.

MATERIALS AND METHODS

Mammalian Cell Culture and Transfection

HEK293 cells (ATCC-CRL-1573; American Type Culture Collection) were maintained in a 95% air/5% CO_2 humidified incubator at 37°C in Dulbecco's modified Eagle's medium (DMEM), supplemented with 0.11 g/L sodium pyruvate, 10% (vol/vol) heat-inactivated fetal bovine serum, 100 U/ml penicillin G, 100 μg/ml streptomycin sulfate, and 2 mM L-glutamine (all from GIBCO BRL). Cells were passaged every 2–3 d (up to 20 times) and were plated on dishes ~24 h before transfection by calcium phosphate-DNA coprecipitation (Sambrook and Russell, 2001). Cells were transfected with cDNAs for the rat α1 GlyR subunit and for the marker protein enhanced green fluorescent protein (EGFP-c1; CLONTECH Laboratories, Inc.) in order to select transfected cells for recordings. Total amount of cDNAs per transfected dish was 2 μg: this quantity was found to give the highest rate of transfection efficiency (~40%; Groot-Kormelink et al., 2002). The cDNA mixture used for the transfection contained 70% of EGFP cDNA, 5% of α1 GlyR subunit cDNA, and 25% pcDNA3.1 vector cDNA (without the α1 GlyR subunit open reading frame). The low proportion of α1 GlyR subunit cDNA was chosen to achieve the right level of expression for single-channel recordings (i.e., minimize the number of patches that had to be discarded because of the presence of too many simultaneous openings of more than one channel; Groot-Kormelink et al., 2002)

Amplification, Cloning, and Sequencing of Full-length cDNAs Encoding Three Different Rat α1 GlyR Subunit Transcripts

A "nested-PCR" approach (Groot-Kormelink and Luyten, 1997) was applied to amplify the full-length coding region of the rat α1 GlyR subunit. Four gene-specific primers were designed on the basis of the published sequence (Akagi, Hirai, and Hishinuma, 1991): Glyα1_5A:CGTTCTCCGGCTTCGTAAGTGCC; Glyα1_3A:GGTGTGTGCTCTTCCTCTCTTCCTCC; Glyα1_5B:GCA*GAATTC***GCCACC**ATGTACAGCTTCAACACTCTGCG; Glyα1_3B:GTA*GCGGCCGC*TCACTTGTTGTGGACGTCCTCTC.

Note that the Glyα1_5B primer has an added Kozak consensus sequence (bold) immediately upstream of the start codon (underlined) and an EcoRI restriction site (italics). Primer Glyα1_3B has a NotI restriction site (italics) immediately downstream of the stop codon (underlined). First round Touch-Down PCR was performed with the primer combination Glyα1_5A/Glyα1_3A for 15 cycles consisting of (a) 1 min at 94°C, (b) 1 min at 68°C, gradually (1°C/cycle) decreasing to 53°C, and (c) 3 min at 72°C. This was followed by 20 additional cycles of (a) 1 min at 94°C, (b) 1 min at 53°C, and (c) 3 min at 72°C. The 50 μl reaction mixture contained 5 μl Rat Brain Marathon-Ready™ cDNA (CLONTECH Laboratories, Inc.), 1.25 U of *Pfu* Turbo polymerase (Stratagene), 0.5 μM of each primer (Amersham Pharmacia Biotech), 1× cloned *Pfu* PCR buffer (Stratagene), and 0.2 mM dNTPs (GIBCO BRL). With 5 μl of the first-round PCR reaction (50× diluted in MilliQ) and the Glyα1_5B/Glyα1_3B primer combination, a second-round nested PCR was performed for 20 cycles of (a) 1 min at 94°C, (b) 1 min at 60°C, and (c) 3 min at 72°C. The composition of the PCR reaction was the same as in the Touch-Down PCR.

Several PCR fragments between 1.3 and 1.4 kb were purified, cloned into the EcoRI and NotI sites of the pcDNA3.1(+) vector (Invitrogen), and sequenced fully on both strands.

Sequence analysis showed that we had cloned three different transcripts for the rat α1 GlyR subunit gene, which we termed the primary transcript, the insertion transcript, and the deletion transcript (EMBL/GenBank/DDBJ accession no. AJ310834, AJ310835, and AJ310836, respectively). All three transcripts have identical sequences except for an insertion of 24 nucleotides at position 1060 for the insertion transcript and a deletion of 128 nucleotides at position 56 for the deletion transcript. The deduced mature protein sequence of the primary transcript is

Published April 29, 2002

100% identical to that of the rat α1 GlyR subunit protein sequence deposited in the Swiss-Prot database (EMBL/GenBank/DDBJ accession no. P07727). The primary transcript was used in this study and shall be referred to as GlyR α1 subunit.

Electrophysiological Recordings

Recordings were performed from transfected cells in the whole-cell patch clamp configuration or in the excised outside-out patch configuration. In both cases, the external solution contained (in mM): 102.7 NaCl, 20 Na gluconate, 4.7 KCl, 2 $CaCl_2$, 1.2 $MgCl_2$, 10 HEPES, 14 glucose, 15 sucrose, 20 TEACl (adjusted to pH 7.4 with NaOH), and the internal contained 107.1 KCl, 1 $CaCl_2$, 1 $MgCl_2$, 10 HEPES, 11 EGTA, 20 TEACl (pH 7.2 with KOH). Both solutions were prepared in HPLC-grade water in order to reduce the effect of contaminant glycine. For whole-cell recordings, 2 mM MgATP was added to the internal solution. Chemicals were from Merck, except for glycine (Fluka).

For whole-cell recording, cells were voltage-clamped at −60 mV with electrodes pulled from thin-walled borosilicate glass (GC150TF; Clark Electromedical) to a resistance between 2 and 4 MΩ. Access resistance was between 4 and 9 MΩ and could be compensated by up to 95% (range 60–95%).

Application of glycine for whole-cell dose–response curves was done with a U-tube system (Krishtal and Pidoplichko, 1980) that allowed exchange times of the order of 15–50 ms (measured using the signal generated by applying a 50% dilution of the bathing medium). Whole-cell current responses to glycine were filtered at 1 kHz, digitized using a CED 1401 interface (Cambridge Electronic Design; sampling rate 5 kHz), and recorded on a computer using the Strathclyde Software for Windows (WinWCP; see http://www.strath.ac.uk/Departments/PhysPharm/ses.htm). The same software was used to determine the peak response for each application of glycine. The resulting measurements were plotted on a semilogarithmic plot and fitted empirically by the Hill equation:

$$y = y_{max}\frac{[A]^{n_H}}{[A]^{n_H} + EC_{50}{}^{n_H}},$$

where y_{max} is the maximum response, EC_{50} is the agonist concentration for 50% maximum response and n_H is the Hill coefficient, using the weighted least squares criterion (CVFIT program, Colquhoun, D., and I. Vais; available from http://www.ucl.ac.uk/pharmacology/dc.html).

Outside-out experiments were performed at a holding potential of −100 mV, using 8–15 MΩ electrodes pulled from thick-walled borosilicate glass (GC150F; Clark Electromedical), coated near the tip with Sylgard® 184 (Dow Corning) to improve their dielectric properties and fire-polished with a microforge (Narishige).

All results are expressed as mean ± SEM.

Single Channel Analysis

Steady-state recordings were obtained with an Axopatch 200B amplifier (Axon Instruments, Inc.), prefiltered at 10 kHz (with the amplifier 4-pole Bessel filter), stored on a DAT tape, then filtered at 3 kHz with a 8-pole Bessel filter and digitized (with the CED 1401 interface) at 30 kHz sampling rate for off-line analysis. The experiments included for analysis had less than 5% of double openings.

All the records were first processed by time course fitting (see Colquhoun and Sigworth, 1995) with the program SCAN to obtain an idealized record containing the duration and amplitude of all the detected events, ready for further analysis by the EKDIST program (both programs by Colquhoun, D., and I. Vais, source as above). A fixed time resolution (30–40 μs for both open and shut times, giving an estimated false event rate below 10^{-20} s^{-1} for the patches selected for analysis) was imposed on each dataset, before the fitting of dwell time distributions by the maximum likelihood method.

Analysis of single channel current amplitudes was performed by fitting mixtures of gaussian components to fitted amplitude distributions. Because of the inevitable uncertainty in assigning an amplitude to short events, only openings longer than two rise-times of the filter were included in the distributions. Thus, the current amplitudes obtained were converted into chord conductances, without any correction for junction potential.

Distributions of open periods, shut times, and burst lengths were fitted with a mixture of k exponentials of the form:

$$f(t) = \sum_{i=1}^{k}\frac{a_i}{\tau_i}\exp(-t/\tau_i),$$

where a_i is the area of the ith component and τ_i is its time constant (Colquhoun and Sigworth, 1995). The results are displayed as distributions of $\log(t)$, with the ordinate on a square root scale (Blatz and Magleby, 1986; Sigworth and Sine, 1987).

Note that an open period was defined as any sequence of openings to one or more conductance levels that does not contain any resolvable shutting.

Bursts of openings were defined as groups of openings separated by shuttings that are all shorter than a specified critical length, t_{crit}. The value of this critical shut time was chosen in order to minimize the total number of misclassified bursts (Jackson et al., 1983). This was achieved by solving for t_{crit} the equation:

$$\frac{a_f}{\tau_f}\exp(-t_{crit}/\tau_f) = \frac{a_s}{\tau_s}\exp(-t_{crit}/\tau_s),$$

where a_s and a_f are the area of the slow and fast component, respectively, in the shut time distribution and τ_s and τ_f their corresponding time constants (the appropriate sums of components were used when more than two were presents). This criterion was chosen because the number of fast and slow events in our distributions were very similar, and in these cases the Jackson criterion minimizes the total number of misclassifications without resulting in excessive fractional misclassification of a small component (Colquhoun and Sakmann, 1985). The number of openings per burst was fitted with a mixture of k geometric components of the form:

$$P(r) = \sum_{i=1}^{k} a_i(1-\rho_i)\rho_i^{r-1} \qquad r = 1, 2, \ldots\infty.$$

All the distributions from each experiment were fitted separately; in some cases (see RESULTS and Fig. 7), burst length distributions obtained in a set of nine experiments (three for each concentration tested) were also fitted simultaneously with the constraint that the time constants be the same for all, only the areas of each component being allowed to vary freely to maximize the likelihood (with the program EKDIST).

Correlation Analysis

Correlation between adjacent open and shut times in some experiments was assessed by several methods (with the program EKDIST). The conditional distributions of the lengths of open periods that were adjacent to shut states with durations in a specified range were fitted. A more synoptic view was given by plotting the means of these distributions against the (mean) adjacent shut time. The analysis of adjacent intervals allowed a visual display of the results as conditional open time distributions. These distributions were determined using both the preceding and fol-

Published April 29, 2002

lowing opening adjacent to a specified gaps. In this way each opening is counted twice, and this approach is justified by the assumption of microscopic reversibility that governs the process of channel kinetics (Rothberg and Magleby, 2001). The closed time ranges for obtaining conditional distributions or mean open times were chosen for each experiment by calculating the critical times between each component of the shut time distribution by means of the same equation used for the determination of the t_{crit} for bursts. Hence, the first range of closed times goes from the time resolution to the t_{crit} between the first and second component in the shut time distribution. The second shut time range varies from the previously calculated t_{crit} to the t_{crit} between the second and third component of the shut times distribution and so on for the remaining ranges.

Correlations between adjacent open times and between burst lengths were calculated using two methods: the runs test and the autocorrelation coefficient, as in Colquhoun and Sakmann (1985).

To apply the runs test, introduced by David and Barton (1962), all intervals (open times or burst lengths) are converted into a series of digits: 0 if the interval is smaller than some critical time (usually 0.3 ms), and 1 otherwise. Defining n_0 as the total number of observed values smaller than the critical time and n_1 as the total number of values above the critical time, we have that the total number of observations (n) is $n = n_0 + n_1$. A run is defined as a series of digits that consists of one (or more) consecutive 0 (or 1) values. If the series is in random order, the mean and variance of the number of runs, T, will be:

$$E(T) = \frac{2n_0n_1}{n} + 1$$

and

$$\mathrm{var}(T) = \frac{2n_0n_1(2n_0n_1 - n)}{n^2(n-1)},$$

respectively.

The variable z, defined as

$$z = \frac{(T - E[T])}{\sqrt{\mathrm{var}(T)}},$$

has a distribution with zero mean and unitary standard deviation, which, for large samples, will be approximately Gaussian.

The autocorrelation coefficient for lag m (r_m) is defined as

$$r_m = \frac{\sum_{i=1}^{n-m}(y_i - \bar{y})(y_{i+m} - \bar{y})}{\sum_{i=1}^{n}(y_i - \bar{y})^2},$$

where the ith of n observations is denoted by yi with corresponding mean $\bar{y}$.

RESULTS

Equilibrium Concentration-response Curves

Transfection of HEK293 cells with rat glycine α1 subunits resulted in the expression of functional homomeric glycine receptors, as demonstrated by voltage-clamp recording in the whole-cell configuration.

Fig. 1 A illustrates the responses to increasing concentrations of glycine obtained from a transfected cell voltage clamped at −60 mV. Slow desensitization is clearly visible for responses to concentrations higher than 50 μM, and in this cell a maximum peak current of ~8 nA is reached at 200 μM glycine.

In the 13 cells tested, the values for the fitted maximum current ranged from 1 to 10 nA with a mean of 4.92 ± 0.89 nA and the Hill coefficient varied between 2.3 and 3.9 (mean 3.3 ± 0.2). The range of EC_{50} values for glycine varied approximately fourfold (from 30 to 120 μM) with an average value of 78.8 ± 7.2 μM.

The wide range of EC_{50} values that we observed is in accord with reports of high variability for the EC_{50} of human (Taleb and Betz, 1994) and zebrafish (Fucile et al., 1999) homomeric α1 glycine receptors expressed in oocytes or Bosc 23 cell lines, respectively. However (see Fucile et al., 1999), the variability in the EC_{50} was not related to the level of surface expression of the receptors. Indeed, as shown in Fig. 1 C, cells with comparable levels of maximum GlyR current can have very different EC_{50}s, and no linear correlation between maximum current and EC_{50} is apparent (Pearson coefficient $r = -0.40$).

Single Channel Currents

In steady-state single-channel recording from outside-out patches (clamped at −100 mV), no openings were detected while the patch was held in control solution, but application of glycine (0.3, 1, 10 μM) elicited channel openings to several conductance levels.

Fig. 2 A shows an example of such openings in the presence of 10 μM glycine. Two levels of conductance are discernible in this portion of the trace: a high conductance of 86 pS and a low one of 40 pS (marked by the two horizontal lines). The slow timescale traces (top row) show that the majority of openings occur at the high conductance level, whereas closer inspection of a record at a faster timescale shows that the events often occur in bursts. Due to the 3 kHz filtering, some of the short openings (or shuttings) do not reach the full amplitude (or the baseline level).

Data in the fitted amplitude histogram (Fig. 2 B) were fitted with two Gaussian components (same patch as in Fig. 2 A). Two Gaussian components were needed in most patches (~60% of a total of 34 patches), whereas the remaining patches exhibited only one (high) conductance level. Note that the two-component fit shown in Fig. 2 B is not very satisfactory, because there are some openings to intermediate amplitudes that are not fitted well. This behavior was seen also in other patches, but the proportion of openings to such intermediate amplitudes was always small (<5%).

The main (most frequent) amplitude was invariably the higher conductance level and this was in the range of 60–90 pS in all experiments. Because of the variability

Published April 29, 2002

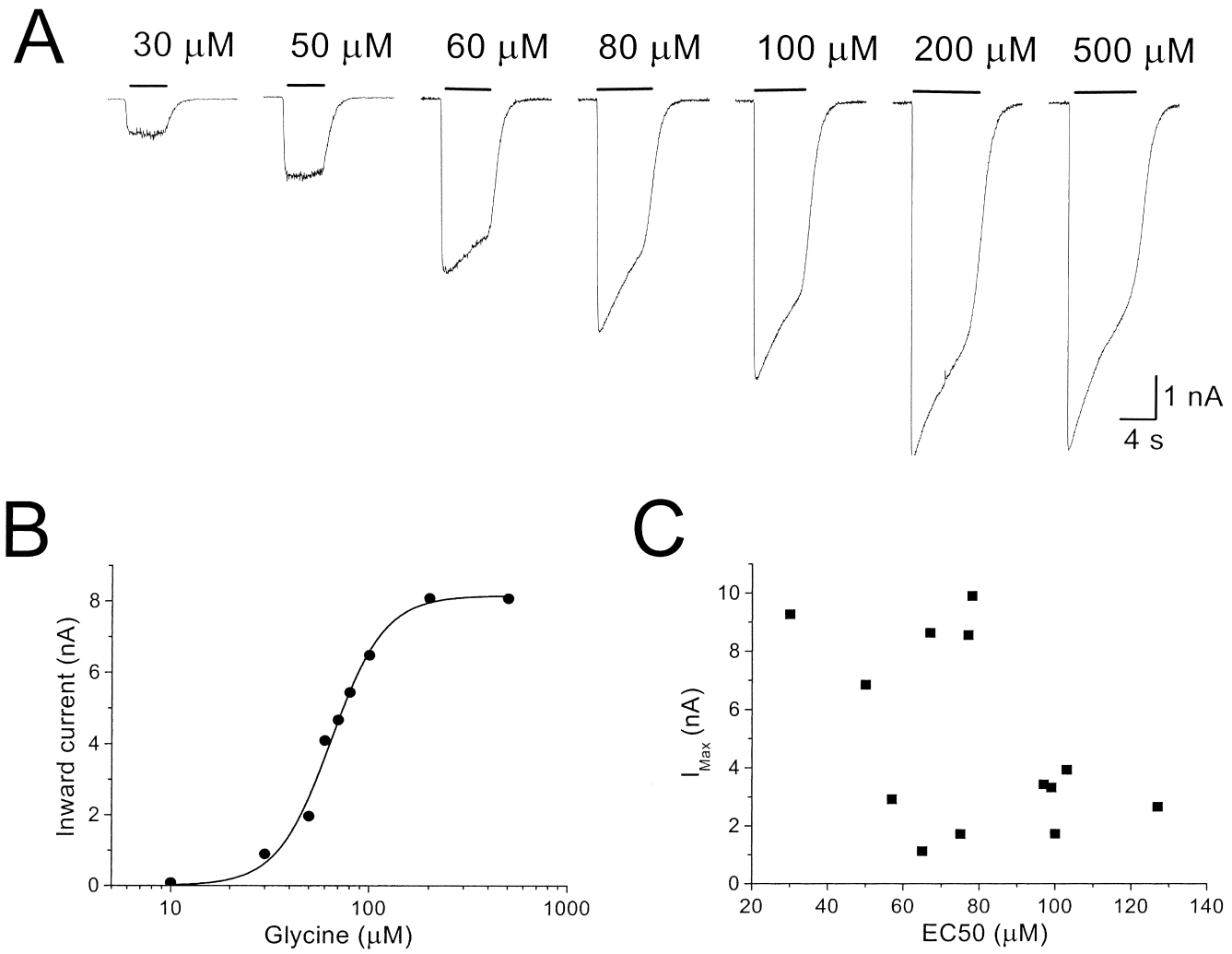

FIGURE 1. Variability of EC_{50} values for whole-cell responses elicited by glycine on HEK293 cells transfected with the rat α1 GlyR subunit. A shows current responses to the application of increasing concentrations of glycine recorded at −60 mV holding potential. Responses increase to a maximum value of ~8 nA for concentrations greater than 200 μM. The full dose-response curve obtained in the experiment of A is plotted in B, where the continuous line is the fit of the Hill equation (here EC_{50} = 64.2 μM, I_{max} = 8.17 nA and Hill slope 3.25). C shows a scatter plot of the EC_{50} values fitted from 13 cells versus the maximum current detected. Linear correlation between the two quantities does not appear to be strong ($r = -0.4$).

of this high conductance level, in some patches this component had to be fitted by two closely spaced Gaussians.

To decide whether to investigate the kinetic behavior of sublevels separately from the main level, we had to detect whether the amplitude distribution is affected by agonist concentration. Thus, we plotted the relative frequency of high and low conductance openings for each concentration. The resulting histogram (Fig. 2 C) shows that low conductance levels account only for ~10% of all the openings, and also that there is no significant difference between the relative frequency of small and high amplitude events at different concentrations. Our data agree qualitatively with the observation by Twyman and Macdonald (1991) that native GlyRs open to two main conductance levels, whose relative frequency does not depend on the concentration of the agonist. However, in our experimental system, lower amplitude openings were a small minority of the total (compare 25% for native GlyRs; Twyman and Macdonald, 1991). Thus, we decided to perform the kinetic analysis of dwell times without distinguishing between the conductance levels. This approximation was not a substantial impediment to our aims, given that the largest conductance level was always predominant.

Properties of Open Periods

Distributions of the lengths of open periods were fitted satisfactorily with a mixture of four exponential densi-

Published April 29, 2002

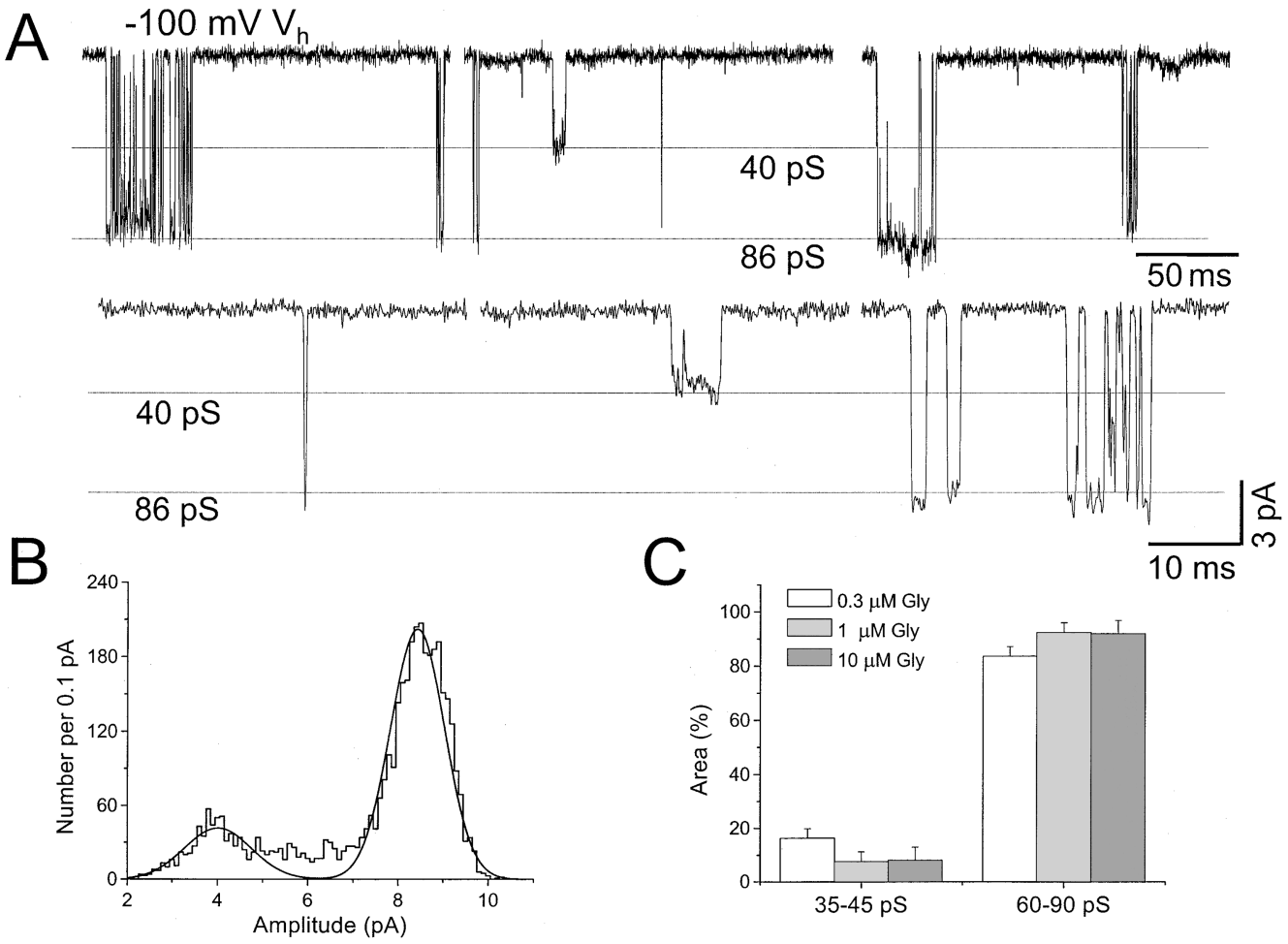

FIGURE 2. GlyR can open to different conductance levels independently of the applied glycine concentration. Downward deflections in the traces in A are examples of openings of GlyR channels elicited by 10 μM glycine in an outside-out patch at −100 mV. Three portions of the record are shown in the top row. Most of the openings occur at a conductance level of 86 pS, but some 40 pS openings were detected as well (top row, middle trace). Events are displayed in the bottom row of A at a faster time scale in order to show the fine structure of bursts of openings for small and large amplitudes. A histogram of the fitted amplitude distribution for the experiment above is shown in B. Data were fitted with two Gaussian curves with peaks at 4.0 pA (1.4 pA standard deviation) and 8.4 pA (1.2 pA standard deviation). The areas under each component were, respectively, 20 and 80%. The histogram in C shows that the average proportion of low (~40 pS) and high (60–90 pS) openings (0.3, 1, and 10 μM, n = 14, 12, and 5, respectively) was not related to agonist concentration. On average, openings to the sublevel accounted for ~10% of the fitted events.

ties for all concentrations tested. Fig. 3 A shows a comparison of open period distributions obtained at three different glycine concentrations. Longer open periods are more frequent with 10 μM glycine, while shorter openings (40–100 μs) occur more frequently in recordings at lower concentrations. This is reflected by the concentration dependence of the overall mean open period, shown in Fig. 3 B (mean calculated from fits as $\Sigma a_i\tau_i$). However, the increase in the mean open period does not result from a change in the values of the time constants that are used to fit the distributions: these time constants do not vary significantly with agonist concentration as shown by Fig. 3 C (bottom; see also Table I). Rather, the change is due to the dependence on glycine concentration of the relative area of each component, as summarized by the bar chart in the top half of Fig. 3 C. This dependence was particularly marked for the areas of the first and the fourth components (namely the faster, $\tau_1 \sim 40$ μs, and the slowest, $\tau_4 \sim 5$ ms). As applied glycine was raised from 0.3 to 10 μM, the area of the first component decreased from 53 to 7%, whereas that of the slowest component increased from 1 to 17%. Roughly speaking, higher concentrations of glycine therefore favor the occurrence of longer openings with respect to short ones, but the "long openings" at high concentrations are not longer, on average, than they are at low concentrations, they are just more frequent. The overall effect is summa-

Published April 29, 2002

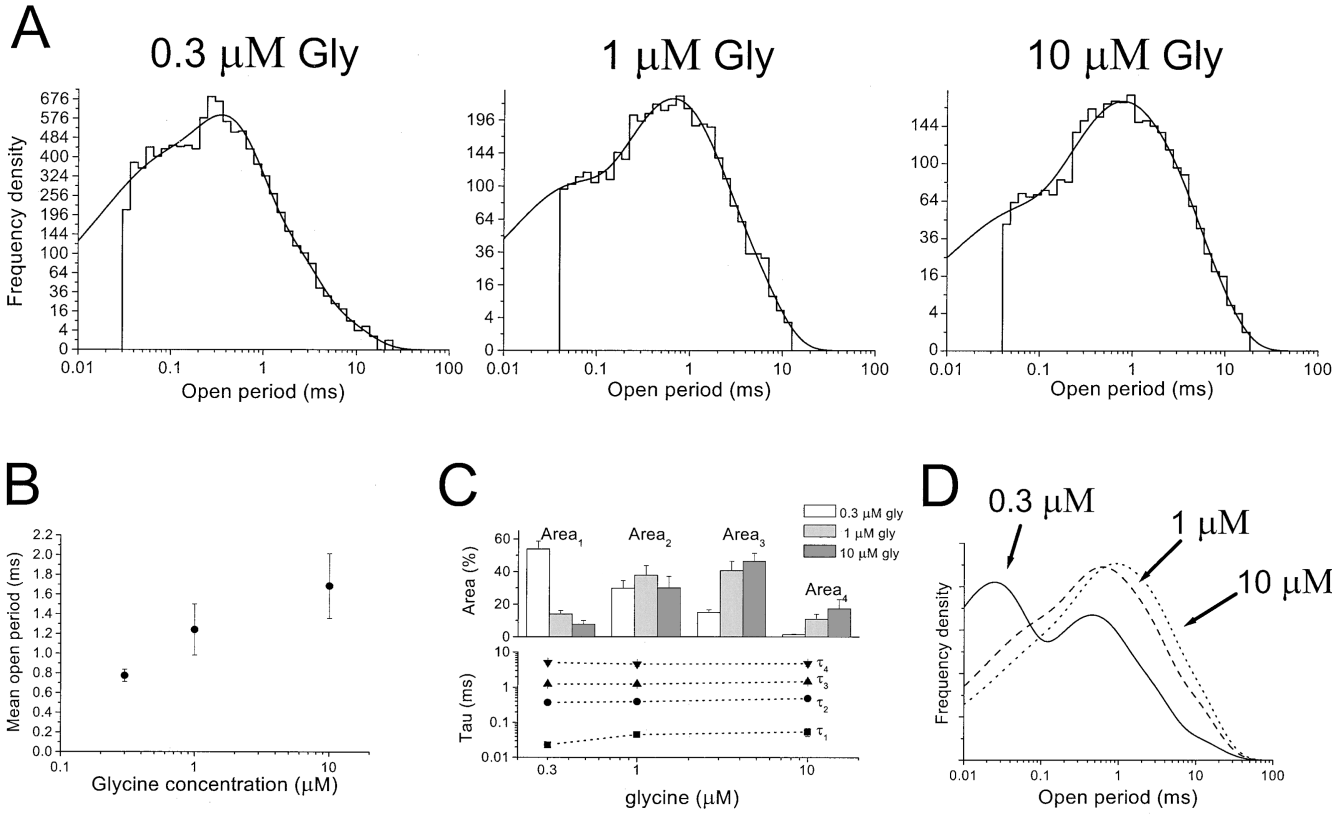

FIGURE 3. The mean duration of apparent open periods increases with agonist concentration. Open period distributions in A were obtained from different patches in response to the application of 0.3, 1, and 10 μM glycine. Time constants were (relative area given in parentheses) $\tau_1 = 0.04$ ms (19%), $\tau_2 = 0.31$ ms (62%), $\tau_3 = 1.1$ ms (17%), and $\tau_4 = 3.1$ ms (2%) for 0.3 μM glycine; $\tau_1 = 0.03$ ms (18%), $\tau_2 = 0.4$ ms (28%), $\tau_3 = 0.8$ ms (37%), and $\tau_4 = 2.1$ ms (17%) for 1 μM glycine; and $\tau_1 = 0.03$ ms (11%), $\tau_2 = 0.4$ ms (31%), $\tau_3 = 1.1$ ms (40%), and $\tau_4 = 2.6$ ms (18%) for 10 μM glycine. The mean open period for all the experiments ($n = 14$ for 0.3 μM, $n = 12$ for 1 μM, and $n = 5$ for 10 μM) is shown in B as a function of concentration (data pooled from all the experiments). C shows that the time constants for the four components vary little with glycine concentration (bottom plot), whereas (top histograms) the areas are strongly concentration dependent. The overall average effect of agonist concentration on open times is shown in D by plotting the multiexponential curves obtained from averaging the τ values and the areas observed for each concentration. The three different curves (each scaled to contain the same number of events) show an excess of short open times for low glycine concentrations.

rized by Fig. 3 D: the curves in this figure were constructed by averaging the time constants and the areas fitted for all experiments at each concentration; distributions were scaled to the same total number of openings. The three superimposed curves show a clear excess of short openings for the average distributions for the experiments at 0.3 μM and an increasing abundance of longer openings for increasing concentrations of glycine.

Properties of Shut Times

The analysis of shut time distributions is useful for two main purposes. The first is to decide the appropriate critical shut time, t_{crit}, for the division of the single

TABLE I

Open Times

Gly	*n*	τ_1	$Area_1$	τ_2	$Area_2$	τ_3	$Area_3$	τ_4	$Area_4$	Mean
μM		*ms*	%	*ms*	%	*ms*	%	*ms*	%	*ms*
0.3	14	0.023 ± 0.002	53.9 ± 4.8	0.37 ± 0.03	29.8 ± 4.7	1.2 ± 0.1	15.0 ± 1.6	5.0 ± 0.7	1.4 ± 0.4	0.77 ± 0.06
1	12	0.045 ± 0.003	14.0 ± 2.1	0.39 ± 0.02	37.8 ± 5.9	1.2 ± 0.17	40.6 ± 5.8	4.5 ± 0.7	10.8 ± 3.2	1.24 ± 0.26
10	5	0.054 ± 0.014	7.8 ± 2.2	0.48 ± 0.04	30.0 ± 7.1	1.4 ± 0.2	46.3 ± 5.0	4.7 ± 0.8	17.3 ± 5.6	1.68 ± 0.33

Average values of the time constants and relative areas for each of the four exponential components that fitted the distributions of open times. The overall mean for each concentration is reported in the last column.

Published April 29, 2002

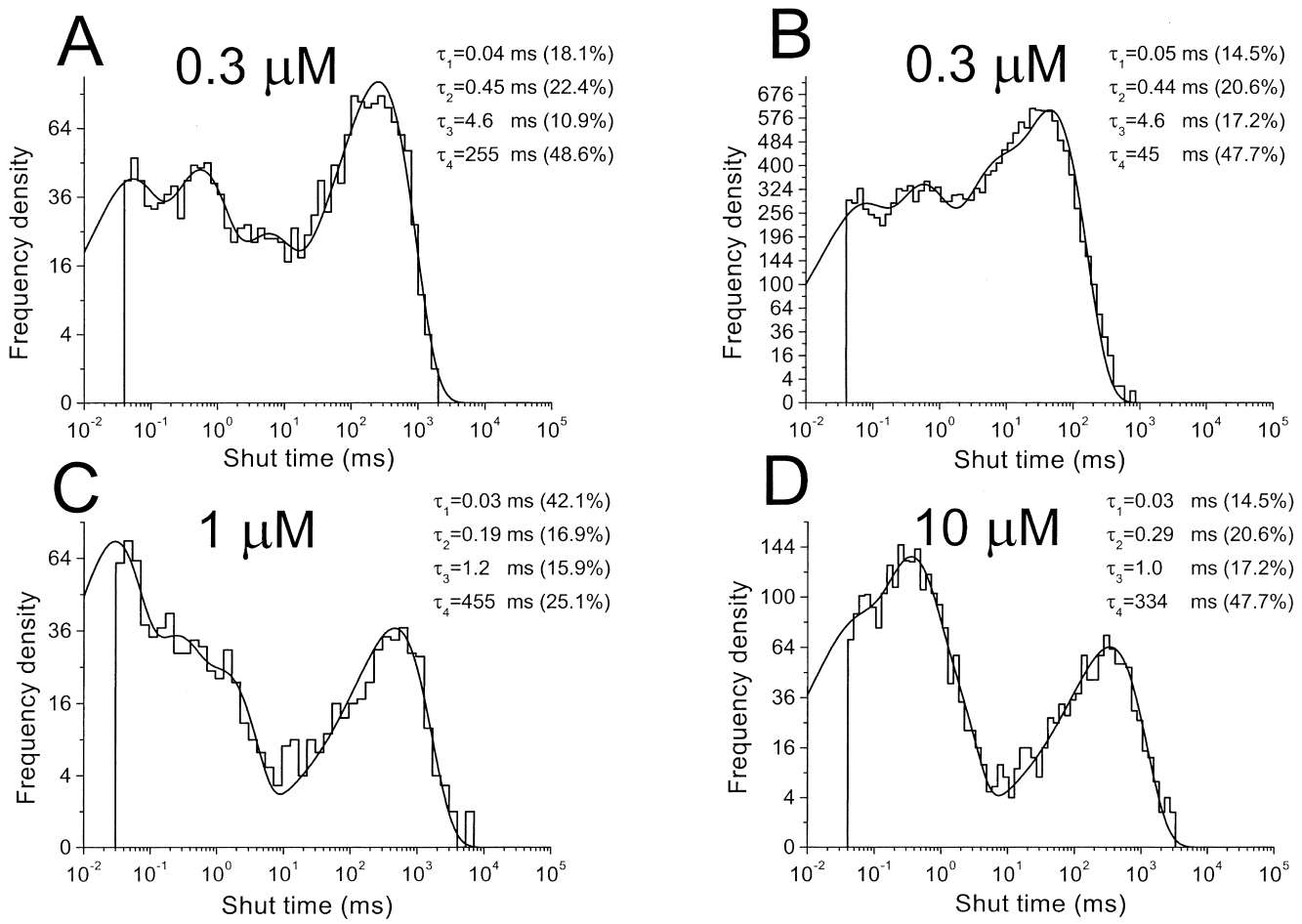

FIGURE 4. Shut times distributions at different glycine concentrations. The shut time distributions were fitted with four exponential components. (A and B) Differences in channel density affect shut time distributions at the lowest agonist concentration. Channel density is low in A, where a good separation is achieved between long and short shut times, but the fit is inaccurate because relatively few observations can be obtained in the life of the patch (see the scale for the number of events on the ordinates). B shows a fit from another experiment, with the same concentration, but with a much higher density of channels in the patch. In this case there are many events (sufficient for burst analysis), but the separation between long and short shut times is less evident. Typical examples from experiments at 1 or 10 μM glycine are shown in C and D, respectively. In both of these cases a good definition of short and long shut times was achieved.

channel record into burst of openings. The second is to measure the short (within an activation) shut times. If these short shut times can be interpreted in the framework of a realistic reaction scheme, these measurements in principle allow us to estimate rate constants for the binding and the gating steps in the scheme. This second matter will be dealt with in the DISCUSSION.

To define t_{crit}, it is necessary to decide which shut times are within a burst (activation; see below) and which are between bursts. The shut times between bursts should depend directly on agonist concentration, since much of the time between bursts is spent in unliganded state(s). It is, however, not easy to see the concentration dependence of the shut times between bursts because in practice they are also affected by the number of channels in the patch. The number of channels in the patch cannot be estimated in our case and, worse still, is likely to vary systematically between experiments at different concentrations. This is because, in order to get a sufficient number of openings at the lowest agonist concentration, it was usually necessary to obtain the data from patches selected to contain more channels than those used for higher concentrations. An example of this is shown in Fig. 4, where the top panels represent shut time distributions obtained in patches from cells with different expression density, A being lower than B (see the *y* axes scale). The patch in Fig. 4 A had good separation of long and short shut times, but few observations, whereas the distribution shown in B had a much larger number of events, but the different components were not so clearly separated.

Published April 29, 2002

TABLE II

Shut Times within Bursts

Gly	*n*	τ_1	$Area_1$	τ_2	$Area_2$	τ_3	$Area_3$
μM		*ms*	%	*ms*	%	*ms*	%
0.3	14	0.057 ± 0.007	42.1 ± 3.7	0.48 ± 0.04	36.0 ± 3.7	4.1 ± 0.5	21.9 ± 3.5
1	12	0.040 ± 0.004	36.1 ± 5.7	0.33 ± 0.03	38.0 ± 4.0	2.8 ± 0.5	25.9 ± 2.9
10	5	0.037 ± 0.005	37.3 ± 5.3	0.38 ± 0.04	48.4 ± 3.1	2.6 ± 0.8	14.2 ± 3.1

Average values for the time constants and relative areas of the three components of the shut time distributions that are deemed to be within bursts.

Fig. 4, C and D, show examples of shut time distributions for 1 and 10 μM glycine, respectively. Four components were used to fit both distributions (see insets for the values fitted to each of the distributions shown and Table II for a summary).

As shown in Fig. 4 A, data from low density patches at 0.3 μM glycine could also be fitted with four shut times, clearly separated. In many of these patches (9 out of 14) a longer shut time component was seen, with a time constant of 1.5 s. Nevertheless, the number of events provided even by the longest recordings from patches with such a low channel density was not sufficient for the reliable fitting of dwell-time distributions, given the several components present. Because of this, we had to use data from patches with higher channel density, despite the poor resolution of the components (see Fig. 4 B and DISCUSSION). Such data were also fitted with four shut time components, for consistency with the data from low density patches at the same concentrations and with the data at higher agonist concentrations.

As shown by the values in Table II, neither the time constants nor the areas of the three shortest shut time components were affected by the agonist concentration in the range 0.3–10 μM.

Burst Analysis

Usually the aim is to define bursts so that they correspond, as closely as possible, to individual activations of the receptor. An activation is defined as the series of (visible) events that occur between the time the first agonist molecule associates with the receptor to the time that the last agonist molecule dissociates (see Edmonds et al., 1995, for a more complete discussion). The idea of a channel activation is important for at least two reasons. First, the proportion of time for which the channel is open during an activation is, in most cases, high enough that one can be virtually sure that the whole activation comes from one individual channel, even when the number of channels in the patch is unknown. Second, it is the summation of individual activations that gives rise to synaptic currents, which are what matters physiologically, and similar time constants can be expected for the time course of synaptic currents and for the distribution of activation (burst) lengths (Colquhoun et al., 1997; Wyllie et al., 1998). A third, practical, reason for wishing to analyze burst lengths rather than open times is that burst lengths are much less affected by errors that result from undetected short shuttings; this means that burst length measurements are more likely than open times to be comparable between different conditions and different labs.

The value of t_{crit} used to define bursts (see MATERIALS AND METHODS) was calculated between the third and fourth shut time components. This calculation was straightforward for the recordings at the higher glycine concentrations, which, as shown by Fig. 4, C and D, had good resolution of the components of the shut time distribution. Average t_{crit} values were 4.6 and 5.8 ms at 1 and 10 μM, respectively ($n = 5$ for both concentrations). The bisection procedure failed for most patches at 0.3 μM with high channel density, as would be expected by inspection of the shut time distributions of such patches (~75% of patches, see Fig. 4 B). Here we chose to use a t_{crit} value of 5 ms (i.e., the average of the t_{crit} at the higher concentrations).

Ideally the separation between the third and fourth components should be 50-fold or more, but this was not always achieved. However, in the experiments with 1 and 10 μM glycine, the percentage of misclassified events was on average only 1.9 ± 0.8%. For the low concentration experiments (0.3 μM glycine), the percentage of misclassified shuttings was 6.2 ± 1.4%, a value perceptibly higher than the one achieved in the experiments at higher concentrations, but still acceptable.

The choice of t_{crit} is complicated by the presence in some patches of an "intermediate" shut time component, with a time constant of 35–65 ms. This component is not seen in records from muscle type nicotinic receptors (Colquhoun and Sakmann, 1985) and it is not obvious whether or not bursts should be defined to contain these shut times. We have chosen not to consider it as 'within bursts' for several reasons. First, this component was observed only in a minority of patches (4/12 and 2/5 of the patches used for burst analysis at 0.3 and 1 μM, none at 10 μM) and, where present, was small in area (<10%). Additionally, the t_{crit} values calculated with this criterion were consistently close to 5 ms both at 1 and at 10 μM. Finally, glycinergic synaptic currents are known to decay quite rapidly (with time constant values in the region of 10 ms; for re-

Published April 29, 2002

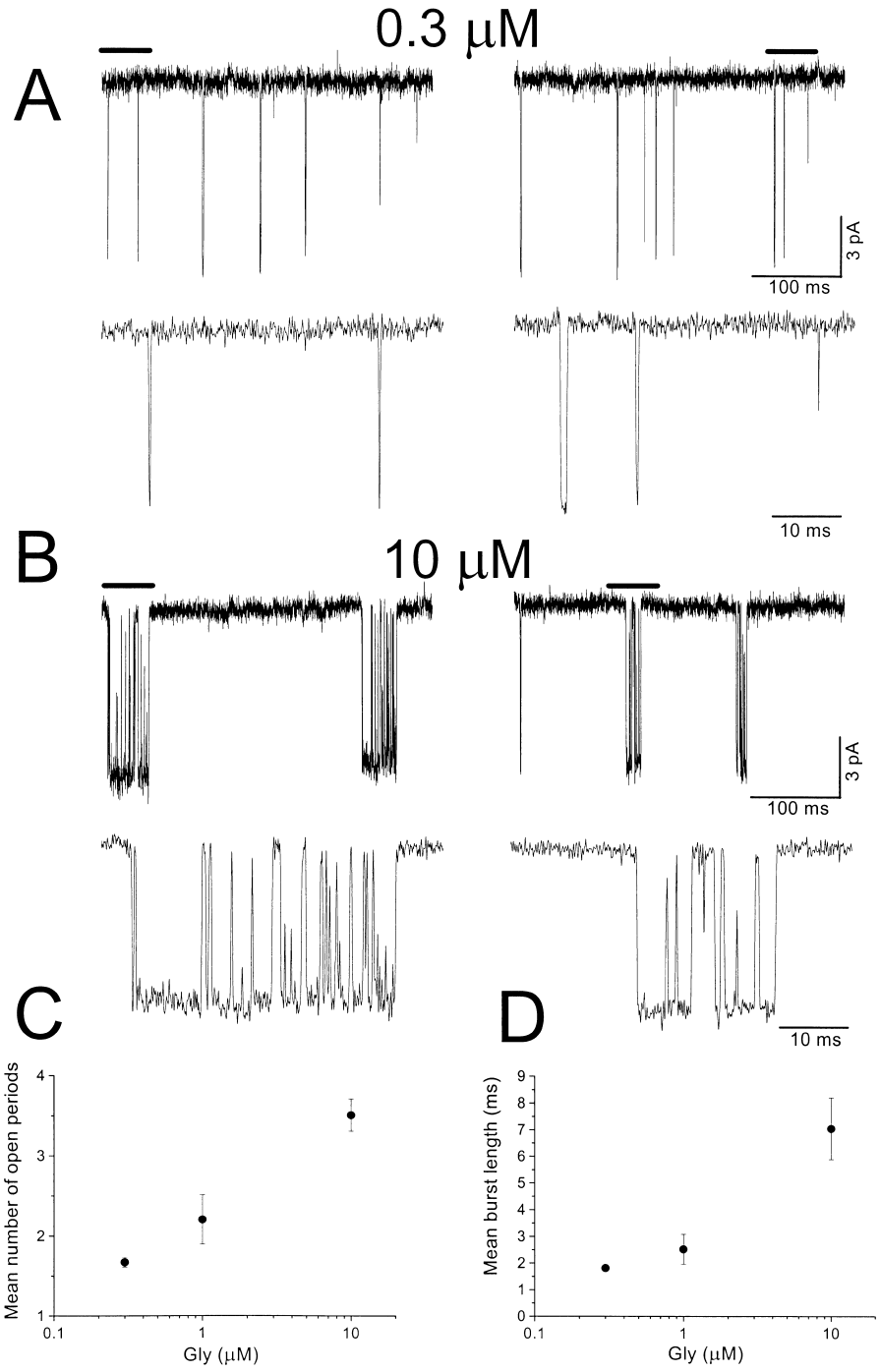

FIGURE 5. Changes in burst structure with agonist concentration. A and B show examples of bursts with 0.3 or 10 μM glycine, respectively. The portions of the trace corresponding to the bar are expanded on a faster time scale in the bottom rows of each panel. While bursts in A are short and often consist of a single opening, bursts at higher concentration of glycine (B) are longer and made up of several openings and shuttings. C shows the increase in the mean number of open periods as a function of concentration. The plot in D shows that the mean burst length increases with increasing concentration of agonist.

view see Legendre, 2001), as do currents elicited by short glycine applications (Singer and Berger, 1999), and it is therefore unlikely that activations would often contain shut times as long as 50 ms. When the analysis was repeated with t_{crit} defined to contain this component, it made little difference to our main conclusions.

Fig. 5 A shows examples of bursts of openings in the presence of 0.3 μM glycine. Activations are short and most of the bursts consist of single openings, as shown on the faster time scale expansion (Fig. 5 A, bottom row). On the other hand, bursts in the presence of 10 μM glycine are much longer (Fig. 5 B) and often contain many openings separated by gaps of variable length (see bottom row).

This trend is summarized by the plot of the mean number of open periods per burst as a function of glycine concentration in Fig. 5 C: the average increases from 1.7 ± 0.1 at 0.3 μM glycine to 3.5 ± 0.2 at 10 μM glycine, confirming that bursts at low glycine are mostly

Published April 29, 2002

TABLE III

Number of Openings Per Burst

Gly	n	n_1	$Area_1$	n_2	$Area_2$	n_3	$Area_3$	Mean
μM			%		%		%	
0.3	14	1.16 ± 0.02	79.2 ± 3.1	3.0 ± 0.3	18.9 ± 2.9	7.7 ± 1.3	5.4 ± 2.1	1.7 ± 0.1
1	12	1.1 ± 0.01	72.5 ± 3.6	2.4 ± 0.1	21.2 ± 3.2	9.6 ± 1.7	6.2 ± 1.2	2.2 ± 0.3
10	5	1.2 ± 0.04	49.8 ± 3.4	3.2 ± 0.4	31.8 ± 2.4	13.0 ± 4.6	18.4 ± 2.7	3.5 ± 0.2

Three geometric components were used to fit the distribution of the number of openings per burst. The mean number of open periods per burst is reported in the last column.

composed of a single opening, whereas bursts at higher glycine concentration have a more complicated intraburst structure.

The distribution of the number of open periods per burst is also potentially informative since it is predicted to be the sum of a number of geometric distributions equal to the number of open states, though there may be fewer components in principle, and/or components with exactly unit mean (see Colquhoun and Hawkes, 1987, for details). In all our experiments only three components were detected in the geometric distribution and the "means" of these components did not depend on the concentration of glycine (see Table III). The two components with higher means describe the presence of bursts with several openings and these are much more frequent with 10 μM glycine, even though these bursts were still detectable at low glycine concentrations. On the other hand, the first component is of particular importance, since its average (at all concentrations) is very close to one and it represents all the bursts that are made up of a single opening. Bursts with a single open period are much more frequent with 0.3 and 1 μM glycine (79 ± 3% and 72 ± 4% of the total number of bursts, respectively), whereas they are only 50 ± 3% of the total for the experiments with 10 μM glycine. However, detection of a component with unit mean is of particular theoretical importance, since it has been shown that this component would be observed also in the presence of a "perfect" time resolution. Furthermore, the existence of this component has also some implications for the classification of the states in a kinetic scheme for the glycine receptor (see Colquhoun and Hawkes, 1987). The observation that bursts at very low agonist concentration are predominantly composed of single or very few openings is also reflected in the concentration dependence of the mean burst length (Fig. 5 D), which increases with agonist concentration from an average of 1.8 ± 0.1 (0.3 μM glycine) to 7.1 ± 1.2 ms (10 μM glycine).

In our case burst length distributions were best fitted by four exponentials in all the experiments with 0.3 and 1 μM glycine. On the other hand, distributions observed with 10 μM glycine always required a fifth component with a longer time constant which was never detected at lower concentrations of agonist. The three examples of such distributions in Fig. 6 A clearly demonstrate the progressive reduction in the number of short bursts with increasing concentration of glycine. This effect is accompanied by an increase in the number of longer bursts. It is again remarkable that the change in the shape of the distribution was not due to a change in the time constants for each component; indeed, the time constants were not significantly different for different concentrations of glycine (see Table IV and Fig. 6 B, bottom graph). However, the relative area of each component was strongly concentration dependent (bar chart, top of Fig. 6 B). The area under the faster component (τ_1) decreased from 57 ± 5% (0.3 μM glycine) to 17 ± 4% (10 μM glycine), whereas the area under the slowest component (τ_4) increased from 2.3 ± 0.4% (0.3 μM glycine) to 17.8 ± 3.1 (10 μM glycine). Furthermore, a fifth component ($\tau_5 \sim 70$ ms) was necessary to fit data adequately at 10 μM glycine. The differences between the three distributions are shown in Fig. 6 C, in which each of the three curves represents a sum of exponential components whose time constant and areas are the averages for all the experiments at a given concentration.

Under certain circumstances (see DISCUSSION) it would be predicted that the time constants (but not the areas) for the burst length distributions should be independent of concentration. This theoretical constraint can be exploited to improve the accuracy of our estimates of time constants and areas of the components of burst length distributions. This is useful, especially since the number of bursts that can be collected from each patch is limited and each fit to a burst length distribution may need up to 10 free parameters. To do this, sets of nine experiments (three for each concentration) were chosen and their burst length distributions were simultaneously fitted with four or five exponential components, constraining the time constants to be identical. Thus, we estimated simultaneously the five common time constants from all the experiments, and the corresponding areas separately for each experiment. Examples of the constrained fits with the nine

Published April 29, 2002

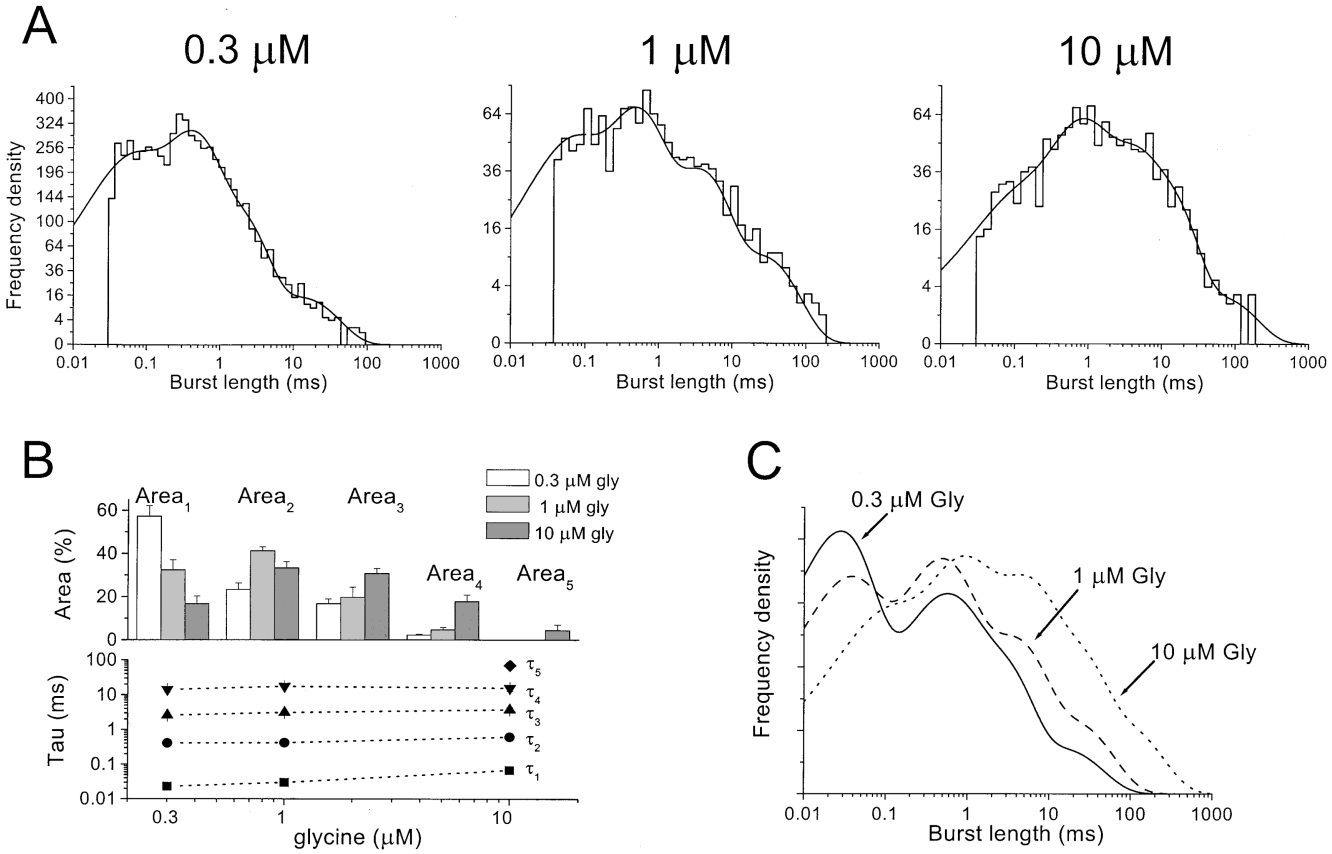

FIGURE 6. The distribution of burst lengths and its concentration dependence. A shows burst lengths distributions from three different patches, one for each of the concentrations tested. The effect of agonist concentration on the average of the fitted parameters for the different components is shown in B. Note (bottom plot) that the average of the five fitted time constants did not change significantly with concentration, whereas the areas of each component (top plot, B) were strongly concentration dependent. The three curves in C were drawn using the average of each parameter (τ values and areas) for each concentration. The three curves show that long bursts are more frequent at high glycine concentrations, whereas short bursts are dominant at lower concentrations.

datasets are shown in Fig. 7 A. In some cases, the agreement of the fitted curves with the experimental data is perceptibly worse when compared with the fit obtained with no constraints, especially for the experiments with a smaller number of observations. However, the average quality of the constrained fits was satisfactory and this procedure has the advantage of taking into account a priori an expected property of the distributions. The curves which resulted from averaging the areas under each component are shown in Fig. 7 B, together with the values of the time constants (indicated by the vertical lines).

This procedure resulted in a more clear-cut concentration dependence of the area of each component when compared with the independent fits. The area of the faster component (τ_1 = 0.03 ms) is now seen to increase from 8 ± 4% (10 μM glycine) to 37 ± 7% (0.3 μM glycine), whereas the slow component (τ_4 = 13.3 ms) decreases from 30 ± 5% for 10 μM glycine to 2 ± 1% at 0.3 μM glycine (see Table V).

TABLE IV
Burst Lengths

Gly	*n*	τ_1	$Area_1$	τ_2	$Area_2$	τ_3	$Area_3$	τ_4	$Area_4$	τ_5	$Area_5$	Mean
μM		*ms*	%	*ms*	%	*ms*	%	*ms*	%	*ms*	%	*ms*
0.3	14	0.023 ± 0.003	57.3 ± 4.9	0.41 ± 0.03	23.4 ± 3.0	2.6 ± 0.2	16.9 ± 2.2	14.1 ± 1.0	2.3 ± 0.4			1.8 ± 0.1
1	12	0.030 ± 0.005	32.4 ± 4.7	0.42 ± 0.02	41.3 ± 1.8	3.1 ± 0.4	19.8 ± 4.7	17.4 ± 1.6	4.7 ± 1.1			2.5 ± 0.5
10	5	0.068 ± 0.003	16.8 ± 3.5	0.62 ± 0.007	33.4 ± 2.9	3.8 ± 0.7	30.9 ± 2.3	15.7 ± 2.7	17.8 ± 3.1	69.3 ± 11.2	4.4 ± 2.6	7.1 ± 1.2

The time constants and their relative areas for the burst length distributions at each concentration. Note that the fifth slowest component was detected only at 10 μM glycine. The overall mean burst length is reported in the last column.

Published April 29, 2002

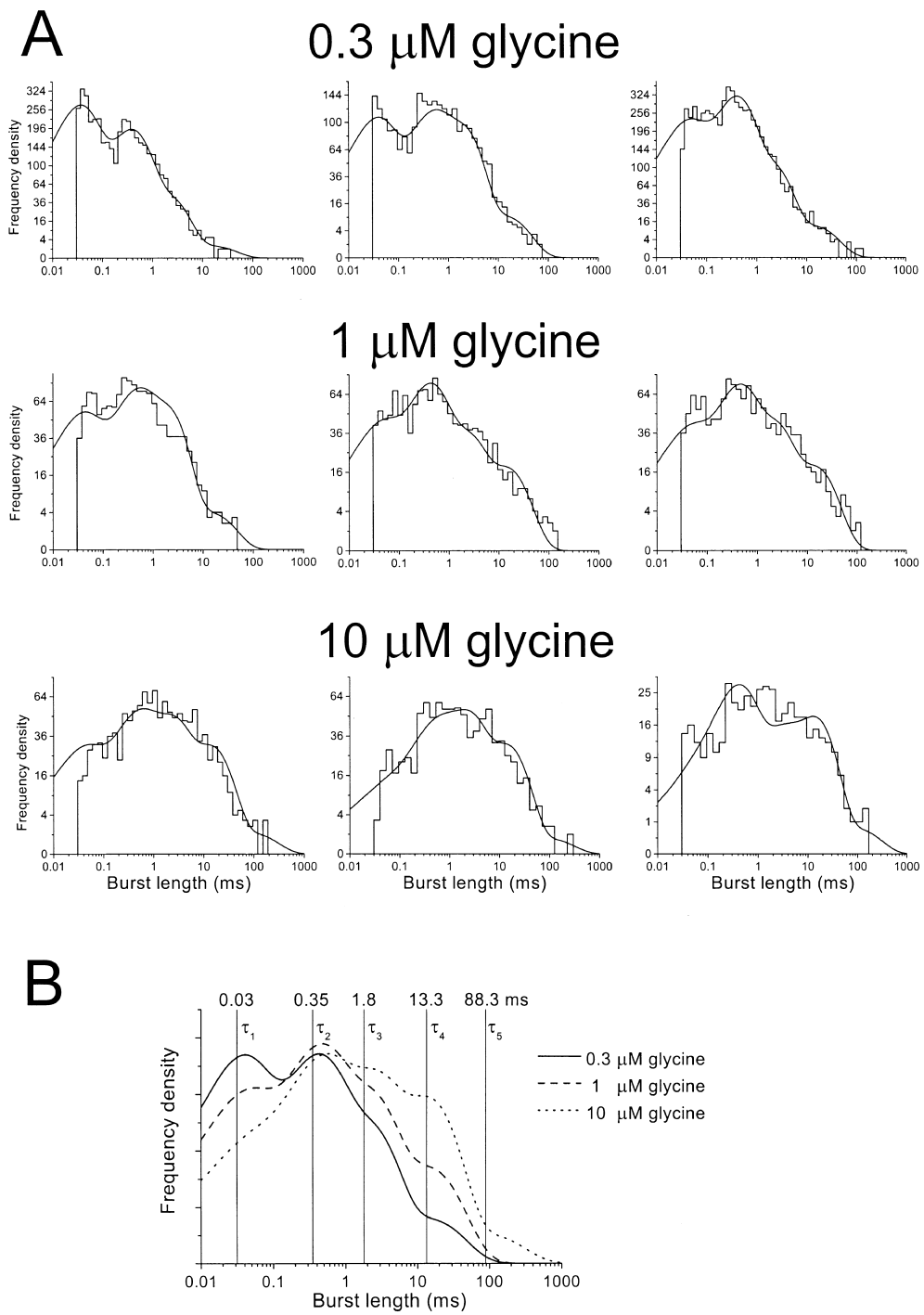

FIGURE 7. Simultaneous fits of burst length distributions from nine patches, with τ values constrained to be equal. A shows data from nine experiments (three for each concentration of glycine that was tested), fitted with the time constants constrained to be the same for all the experiments. The curves drawn in B were drawn using the fitted τ values and average area for each concentration. Vertical lines mark the values of the time constants for each exponential component.

Distribution of Open Times Adjacent to Gaps of Specified Length

The existence of correlations between the length of an opening and that of the following or preceding shut times can provide valuable information about the connectivity of the various states of the receptor. Such correlations have been observed in several different ion channels (see Colquhoun and Sakmann, 1985; McManus et al., 1985).

Fig. 8 A shows distributions (for 0.3 μM glycine) of the lengths of open periods, including either only the open periods that are adjacent to short shut times (Fig. 8 A, left), or only those that are adjacent to long shut times (Fig. 8 A, right). In these examples, a "short shut time" is defined as a shut time shorter than the t_{crit} for the definition of bursts (see above). In the patch in Fig. 8 A, this corresponds to a range between 30 μs (the time resolution) and 6 ms. In the same patch, shut

Published April 29, 2002

TABLE V

Burst Lengths (τs Constrained)

Gly	*n*	$Area_1$ (τ_1 = 0.031 ms)	$Area_2$ (τ_2 = 0.35 ms)	$Area_3$ (τ_3 = 1.8 ms)	$Area_4$ (τ_4 = 13.3 ms)	$Area_5$ (τ_5 = 88.3 ms)
μM		%	%	%	%	%
0.3	3	37.7 ± 6.7	38.5 ± 6.4	21.6 ± 7.4	2.1 ± 0.9	
1	3	21.8 ± 2.7	38.2 ± 3.7	30.1 ± 4.7	10.0 ± 3.7	
10	3	7.8 ± 4.4	30.5 ± 6.9	30.4 ± 7.4	30.4 ± 3.1	1.4 ± 0.2

Burst length distributions from nine experiments were simultaneously fitted constraining the τs to be the same for all the experiments and concentrations. The estimated areas for each concentration and the common values for the time constants are reported. Note the sharp concentration dependence of the areas.

times between 6 ms and 3 s in duration were classified as "long".

The resulting two histograms differ in the number of long and short openings: in fact, short openings are more likely to occur after a long shut time and long openings occur more often after a short shut state. It would be expected for a Markov process that the time constants would be the same for the conditional distributions as for the overall distribution, whereas only the areas are expected to differ (Colquhoun et al., 1996). Indeed, we found that fitting the two conditional distributions with the time constants free to vary gave time constant estimates that were not significantly different from those obtained in the fitting of the overall distribution of all open period durations (unpublished data). Therefore, the conditional distributions were refitted with time constants fixed to the values obtained from the corresponding fits to unconditional open period distributions. Examples of such fits are given by the solid lines in Fig. 8 A, in which four exponential components were used (time constants 0.043, 0.32, 1.20, and 4.81 ms). The relative areas for each component were different for the two distributions: in the distribution of open times adjacent to short shut times, the two faster components had areas of 10.7 and 61.5%, whereas the slower two had areas of 26.1 and 1.7%. In the distribution of open times adjacent to long shut times, the faster components had larger areas (27.8 and 64.4%) and the slowest ones had smaller areas (7.6 and 0.2%). Differences between the two distributions are more evident when they are compared by superimposing the two fits, as in Fig. 8 A, where the dashed line in the distribution in the left panel is the fit to the conditional distribution in the right panel; each fit is scaled to the same number of observed events as the continuous line. A similar pattern is observed with higher glycine concentrations (see the examples in Fig. 8 B for 10 μM glycine). Here the t_{crit} was 1.5 ms and therefore the panel on the left shows open times adjacent to gaps between 30 μs and 1.5 ms, with open times adjacent to shut times between 1.5 and 3000 ms in the right panel. The two distributions were fitted with four exponential components (time constants 0.08, 0.61, 1.9, and 6.3 ms, solid lines). The areas of each component are 1.5, 48.5, 47, and 3% for the distribution of open times adjacent to short shut times, and 14.2, 70.5, 14.5, and 0.8% for the open times adjacent to long shut times. Again, in each histogram, the fit to the distribution in the other histogram is shown as a dashed line.

The procedure of fitting the conditional distributions of open times has the disadvantage of requiring a large number of events to have an accurate fit of each of the distributions. An alternative way of obtaining an overall picture of the presence of correlations is to examine not the distribution, but the mean length of open periods that are adjacent to shut times in specified ranges (Blatz and Magleby, 1989; Gibb and Colquhoun, 1992). Openings adjacent to shut times in five different ranges (defined to correspond to the shut time components, see MATERIALS AND METHODS) were averaged and their mean value was normalized and expressed as a percentage of the overall mean open time in each experiment. The percentages were then pooled and averaged for all experiments at each concentration. The results obtained with this approach are shown in Fig. 8 C: the mean open times adjacent to a specified closed time range are plotted against the mean of the closed times in that range. There is a clear negative correlation between open and closed times at all the three concentrations tested, such that open times longer than average are adjacent to the shortest shut times and vice versa.

Correlations between Apparent Open Periods and Burst Lengths

Further information about connectivity in the mechanism can be obtained from the correlations between the lengths of consecutive events of the same type, namely open periods, shut times, or bursts. For all these quantities, measurements of runs and of autocorrelation coefficients were made (see MATERIALS AND METHODS). Both of these measurements are affected by missed gaps within bursts; furthermore, the correlation coefficients for burst lengths are not easily interpret-

Published April 29, 2002

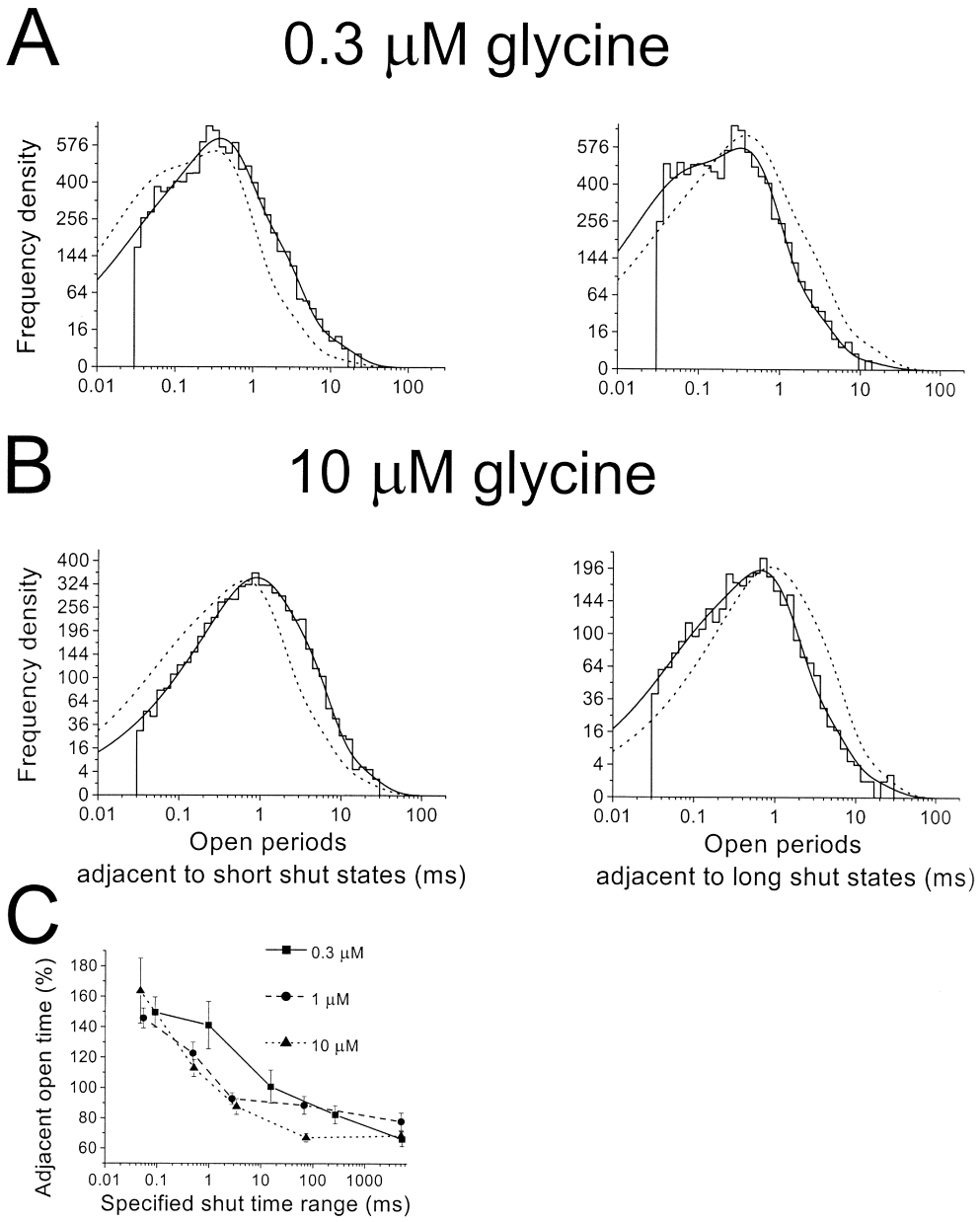

FIGURE 8. Correlation of apparent open periods and shut times. (A) Conditional distributions of open times adjacent to short (left histogram) or long (right histogram) shut states during steady-state application of 0.3 μM glycine. The continuous line is the fit to the data shown in the histogram and the dashed lines in each plot show the corresponding fit of the histogram of the opposite column (scaled to contain the same number of observation as the experimental data). The same conditional distributions for an experiment with 10 μM glycine are shown in B. The difference between continuous and dashed lines show the excess of short (long) openings occurring adjacent to long (short) shut states for both concentrations. (C) Pooled data from experiments with 0.3 μM (n = 14), 1 μM (n = 12), and 10 μM (n = 5) glycine. The plot shows the relationship between the mean duration of adjacent open and shut intervals. The conditional mean open period is expressed in percentage of the overall mean open period for each experiment and such percentages were averaged for each shut time interval (chosen to correspond with the components of the shut time distribution). For the three concentrations tested, the mean apparent open period decreased with increasing range of shut times.

able given the lack of knowledge of the exact number of channels in the patch.

Open Periods

Correlations between open periods were detected at all the three concentrations tested. The runs tests with a critical value of 0.3 ms gave a standard deviate (see MATERIALS AND METHODS) of $z = -6.1$, -4.4, and -4.1 for 0.3, 1, 10 μM glycine, respectively. This is a good evidence for the presence of runs of short (<0.3 ms) and long (>0.3 ms) apparent openings. This is confirmed also by inspection of the correlation coefficients for the three increasing concentrations of glycine (r_1 = 0.10, 0.14, 0.18, respectively). Correlation coefficients were calculated for lags up to 20: as expected, correlations become small for lags greater than four.

Burst Lengths

Correlations between burst lengths are potentially informative (Colquhoun and Hawkes, 1987), but they cannot be measured here because we don't know how many channels are in the patch. It is not possible to know whether two consecutive bursts are generated from the same channel or not. We observed no correlations between burst lengths at 10 μM glycine ($z = -0.6$ and $r_1 = 0.034$). However, small but significant correlations were observed for the experiments with 0.3 and 1 μM glycine, with z values of -4.4 and -2.1, respec-

Published April 29, 2002

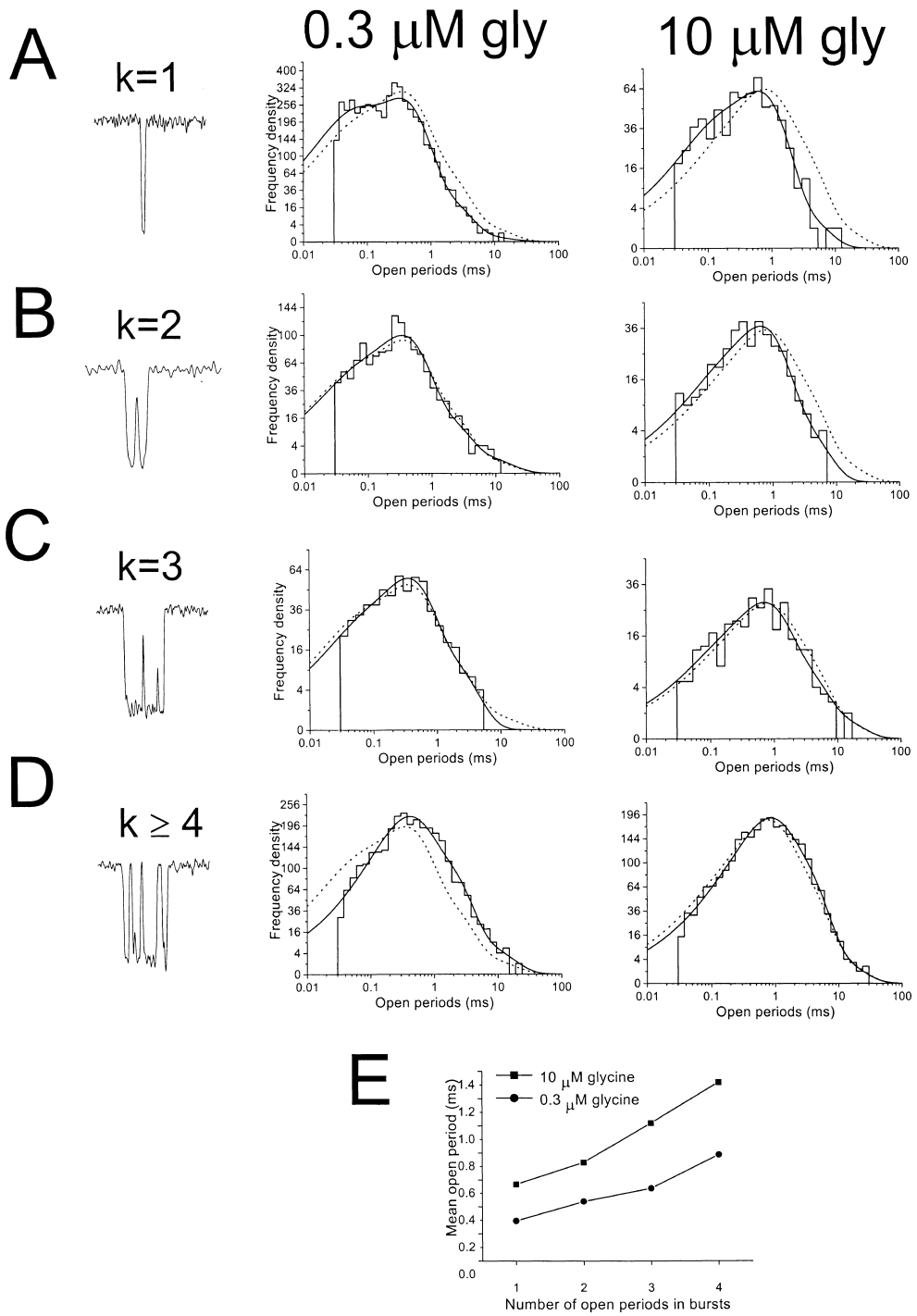

FIGURE 9. The structure of bursts: bursts with one opening contain openings shorter than average. Open period distributions were restricted to include only open periods occurring in bursts containing k openings. Open periods occurring in bursts with k = 1, 2, 3, or ≥4 openings are shown in A–D for two patches exposed to 0.3 and 10 μM glycine. The corresponding fits for the distribution of all the open times (dashed lines) are superimposed to the fit of the open times in bursts with k openings. The difference between the two curves in each plot shows that longer open periods occur more frequently in bursts with a greater number of openings. This is shown also in the plot of E, in which the mean open period increases as a function of the number of opening in the bursts (data refers to the same two patches as in A–D).

tively. Also, the values of the r_1 coefficient (0.11 and 0.12) were indicative of some correlation.

The Structure of Bursts: Open Periods in Bursts with a Defined Number of Openings

The distribution of the number of apparent open periods per burst shows that many bursts (79, 73, and 50%, respectively, for 0.3, 1, and 10 μM glycine; see Table III) comprise a single opening and that the component with unit mean is more prominent at low concentrations. From the burst length distribution we already noted that there is an exponential component, with ~0.03 ms time constant, whose relative weight is highest at the lowest agonist concentration (i.e., short bursts are more frequent at low glycine concentration). This suggests that the short bursts usually do not contain gaps.

It is important to ascertain not only whether short bursts and long bursts differ in the number of openings

Published April 29, 2002

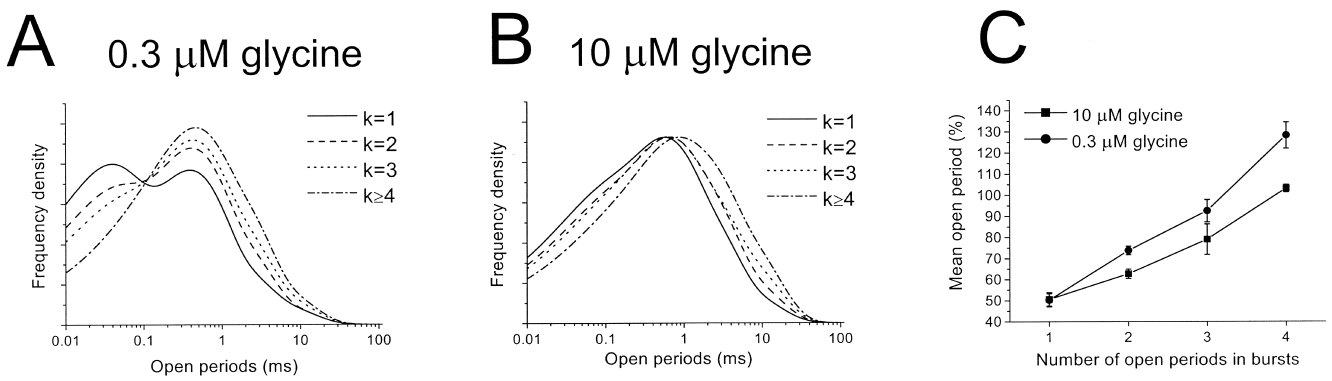

FIGURE 10. Open periods in bursts with k openings. A and B show the results from $n = 4$ and $n = 3$ experiments with 0.3 and 10 μM glycine, respectively. The four curves are obtained by averaging the parameters for the open time distributions for open periods taken from bursts with k openings. For both concentrations, comparison of the curves shows that bursts with 1 or 2 openings contain much shorter open periods than bursts with 3 or ≥4 openings. This is also reflected in the mean open period as a function of the number of openings per burst, plotted in C. In this plot the mean open period is expressed as percentage of the overall mean open period for each experiment.

they contain, but also if they differ in the duration of such open periods. This was done by comparing the distribution of all apparent open times with the distribution of the open times restricted to bursts that contain only a defined number of open periods. This is shown in Fig. 9 A for bursts that have one opening at 0.3 and 10 μM glycine, respectively. The two distributions were fitted with four exponential components, constraining the time constants to be the same as those fitted in the overall distribution of these patches. The dashed lines show the scaled fits to the overall open period distribution in the same patch. There is an excess of short openings among open periods that occur in bursts with only one opening ($k = 1$): the area of the fastest open component detected represents a higher proportion of the open periods in bursts of one opening than in the overall open period distribution. This is true at both ends of the agonist concentration range that we tested, as the shortest component represented 31 and 20% of openings in bursts with $k = 1$ (at 0.3 and 10 μM glycine, respectively, see continuous fitted lines), but only 19 and 6% of all the open periods (for the same patches and concentrations; Fig. 9 A, see dashed lines). Because the time constant of this component is so short and close to the resolution limit in our recordings, our figures may be substantial underestimates of these areas. These data show that short openings are over-represented in bursts with a single open period. Conversely, if this is true, longer open times should be more frequent in bursts with several openings. This is shown by the other distributions in Fig. 9, which show that the excess frequency of short open times decreases as the number of openings goes from $k = 1$ to $k = 3$. When open periods appearing in bursts with more then four openings are considered, an excess of longer open times is seen at both the concentrations tested.

Note that the greatest differences between the constrained distributions and the overall distribution are seen at 10 μM glycine for bursts with one opening and at 0.3 μM for bursts with four or more openings. This is simply because at 0.3 μM most of the bursts consist of one opening and the conditional distribution is close to the unconstrained overall distribution.

A plot of the mean open period for bursts with 1, 2, 3, and ≥4 open periods is shown for the above experiments with 0.3 and 10 μM glycine in Fig. 9 E. The means of the open period for all the detected openings in these two patches were 0.57 ms and 1.15 ms for 0.3 and 10 μM glycine, respectively.

Fitting the distributions of open periods taken from bursts with a fixed number of openings can be done only in patches with a large number of events, if an accurate estimate of the area under each component for each subset of data is to be obtained. All the experiments in which this approach was possible ($n = 4$ for 0.3 μM glycine and $n = 3$ for 10 μM glycine) were pooled together to give an estimate of the change in the area of each of the components underlying the open period distribution. Fig. 10 A shows the distribution curves obtained averaging the areas ($n = 4$ experiments) of each component for any given k. Open periods taken from bursts with increasing number of openings are shifted toward longer values, whereas most of the isolated openings are short. The same observations apply for the three experiments with 10 μM glycine in which this analysis was possible (Fig. 10 B). Results from all the experiments were also pooled to give the plot of Fig. 10 C, in which the mean open period for events taken from burst with k openings, is normalized and expressed as percentage of the overall mean open period.

DISCUSSION

The ultimate aim of our work is to obtain a quantitative model for the activation of the glycine receptor. We shall

Published April 29, 2002

consider now how far toward this goal we get with our results on the steady-state behavior of the homomeric α1 glycine receptor at a range of low agonist concentrations.

Conductance Levels

The main conductance level was observed was in the range between 60 and 90 pS. A second, less frequent level (~10% of events) had 40 pS conductance and was observed only in ~40% of the patches. Although this is a surprisingly wide range (much broader than is observed for muscle nicotinic, or even NMDA, receptors), the highest level of 60–90 pS is in agreement with all the published work on homomeric α1 glycine receptors, irrespective of the expression system (see Bormann et al., 1993) and of whether the expressed clone comes from rat, human, or zebra fish (the sequence of the major pore-lining domain, M2, is the same in the α1 subunits of all these species). A greater discrepancy between different labs is seen in the number of different conductance levels reported (up to eight; Moorhouse et al., 1999). This may be due to several reasons, some related to our choice to analyze the data by time course fitting rather than by a threshold crossing method. It was clear that some openings, especially the lower amplitude ones, are quite "wobbly" and often do not have well-defined amplitudes (as occurs also with neuronal nicotinic receptors). Such openings would cause havoc with any attempt to define the number of conductance levels by means of predefined amplitude windows as needed for threshold-crossing analysis: openings would cross several window boundaries, but the "number of levels" would be defined by the windows, not by the data. On the other hand, time course fitting programs (like SCAN, used here) estimate each amplitude without preconceptions.

In the present study, the aim of the analysis of the conductance levels present was simply to decide whether we should perform a separate analysis of the two distinct conductance levels, as in Twyman and Macdonald (1991). Since openings to the small conductance level were relatively uncommon and their frequency was independent of the concentration of agonist, we chose to pool such events together with openings to the main conductance. It is unlikely that these low conductance openings come from an endogenous channel, since in control solution no openings of any amplitude were detected.

Direct transitions between the sublevel and the main level were never observed, thus raising the possibility that low conductance openings come from a distinct population of glycine-activated channels, whose level of expression is very low (given that small openings were not seen in >50% of the experiments). This hypothesis of two distinct channels is, however, made unlikely by our observation of openings to different conductances occurring in the same burst, i.e., transitions between the two conductance levels separated by a very short gap. It is thus possible that the low conductance level is a rarely visited state of the same glycine receptor that opens mostly to 60–80 pS.

The Number of States

In the attempt to establish a kinetic scheme for the homomeric glycine receptors, some information on the minimum number of states can be extracted from the number of distinct components in the distributions of the observed quantities (such as open periods, shut times, or burst lengths). It is also necessary to consider what number of binding sites is plausible on the basis of what we know of the molecular structure of glycine receptors. There are potentially five binding sites on a homomeric pentamer, irrespective of whether the binding site for glycine is located within the α subunit or at the interfaces between subunits. The question now becomes whether all of these sites can be occupied by glycine and whether the channel can open efficiently from states that are not fully occupied. Another clue comes from the high value (3.3 ± 0.2) of the Hill coefficient observed in whole cell recordings (in agreement with published values up to 4.1–4.2, see Bormann et al., 1993; Taleb and Betz, 1994). This value suggests that there are more than three binding sites and that channels may open when more than three molecules of glycine are bound.

Open Periods

The open period distribution always had four distinct exponential components (rather than the three components reported in GlyR single channel literature; see Twyman and Macdonald, 1991; Takahashi et al., 1992; Fucile et al., 1999; Laube et al., 2000). The additional component reported here has a time constant of ~40 μs, at least fivefold shorter than the fastest open period component detected in previous experiments on homomeric glycine receptors (Takahashi et al., 1992; Fucile et al., 1999; Laube et al., 2000). Its detection is simply due to the improved time resolution in the present series of experiments. An overall improvement in resolution is also likely to be the reason for the small differences between our estimates of the other open period time constants and those previously described: this is because missing fewer short shut times leads to a smaller distortion of the open period distribution.

The most straightforward interpretation for the existence of four distinct components is the presence of at least four different open states of the receptor.

Analysis of open periods showed that the time constants of each exponential component did not change detectably with increasing agonist concentration in the range tested. On the other hand, the areas of these components were strongly affected by glycine concentration: faster events were much more frequent at low

Published April 29, 2002

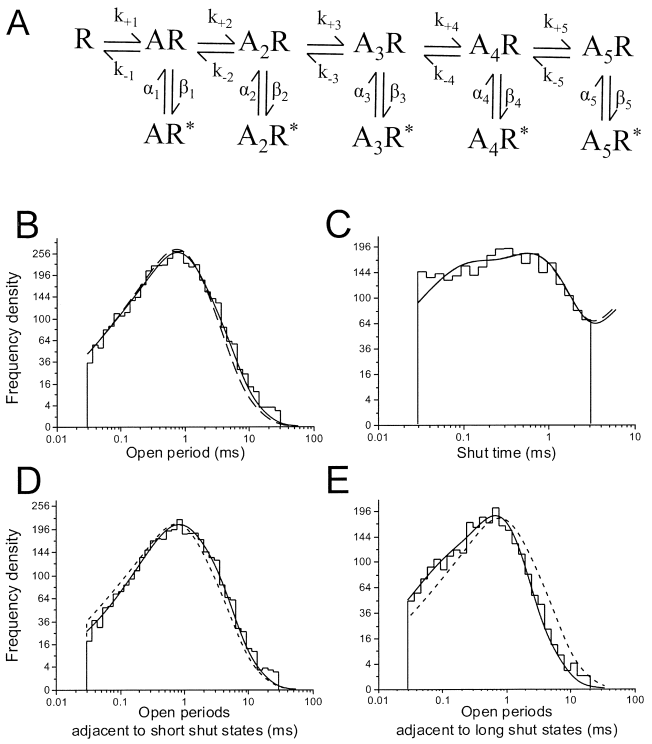

F

Rate	Value	Coeff. Variation (%)	
α_1	22409	23	E_1=0.006
β_1	82	40	
α_2	1740	10	E_2=0.7
β_2	1149	26	
α_3	2047	21	E_3=1.7
β_3	2358	34	
α_4	1094	22	E_4=21
β_4	22444	25	
α_5	294	17	E_5=17
β_5	4663	26	
k_{-5}	4464	82	$K_5=33\times10^{-6}$
k_{+5}	1.84×10^{8}	77	
k_{-4}	8781	25	$K_4=20\times10^{-6}$
k_{+4}	2.23×10^{8}	39	
k_{-3}	534	18	$K_3=10\times10^{-6}$
k_{+3}	1.04×10^{8}	37	
k_{-2}	4876	43	$K_2=56\times10^{-6}$
k_{+2}	4.90×10^{8}	60	
k_{-1}	2744	52	$K_1=62\times10^{-6}$
k_{+1}	5.00×10^{7}	0	

FIGURE 11. Results of the direct fit of a plausible mechanism to the sequence of events. A shows the mechanism fitted. B and C show open and shut time distributions of an experiment at 10 μM glycine. The solid line superimposed on the histogram is the HJC open period distribution calculated from the fitted rate constants, taking into account the experimental time resolution (30 μs), whereas the dashed line is the distribution expected if there were no missed events. Note that the shut time distribution is fitted only up to t_{crit} (3 ms in this case). D and E show open times conditional distributions for the same patch, namely open periods adjacent to shut states shorter (D) or longer than 3 ms (E; compare Fig. 8). F shows the averages of the rate constants obtained by fitting the scheme in A to the data of nine patches (three patches at each of the concentrations tested of 0.3, 1, and 10 μM). The other columns show the coefficient of variation of the fitted parameters and, for reference, the corresponding dissociation constant (K, expressed in M) and efficacy ($E = \beta/\alpha$) for each of the states of ligation. Rate constants are expressed in s^{-1} or $M^{-1}\,s^{-1}$ as appropriate.

concentration of glycine, whereas longer events became dominant at higher concentrations. This phenomenon was first described for glycine receptors by Twyman and Macdonald (1991) in mouse cultured spinal neurons, and by Fucile et al. (1999) in zebrafish recombinant homomeric receptors. Our results extend theirs to a wider concentration range (~30-fold).

This observation is not unexpected on the basis of single channel theory. In principle, there are two ways in which agonist concentration can affect the distribution of open times, which is given in its general form by

$$f(t) = \phi_o \exp(\boldsymbol{Q}_{AA} t)(-\boldsymbol{Q}_{AA})\boldsymbol{u}_A,$$

where the initial (row) vector, $\boldsymbol{\phi}_o$, contains the probabilities that an opening starts in each of the open states, $\boldsymbol{Q}_{AA}$ is the part of the $\boldsymbol{Q}$ matrix of transition rates that corresponds to the open states, and $\boldsymbol{u}$ is a unit column vector (see Colquhoun and Hawkes, 1982, 1995). The time constants for the distribution of open times (in the absence of missed events) come from the eigenvalues of $\boldsymbol{Q}_{AA}$ and are not expected to depend much on concentration. This is because at low concentrations, as used here, $\boldsymbol{Q}_{AA}$ depends little on concentration. Note that $\boldsymbol{Q}_{AA}$ is not at all concentration dependent in the case of schemes like that shown in Fig. 11 A, in which there are no direct connections between open states with different numbers of agonist molecules bound. On the other hand, the areas associated with each time constant in the open time distribution are heavily influenced by the initial vector, which is expected to be strongly dependent on concentration when the different open states have different numbers of ligands bound.

Shut Times and the Choice of t_{crit}

Shut times distributions were fitted with four exponential components. The first three time constants were relatively stable at the different concentrations of gly-

Published April 29, 2002

cine. These results were broadly consistent with those of Twyman and Macdonald (1991), Fucile et al. (1999), and Laube et al. (2000). In particular, the values of the time constants for the second and third of the components we observed (0.3–0.5 and 2.6–4 ms, respectively) are in reasonable agreement with those of the two short (within burst) components described previously (which were in the range of 0.2–0.3 ms and 1.1–2.4 ms for homomeric recombinant glycine receptors). Additionally, we detected a shorter component (time constant around 0.04 ms).

There is also agreement in choosing a t_{crit} for the definition of bursts (activations) that is longer than the first three shut time components. Our t_{crit} value of 5 ms is similar to values of 1.9–4.9 ms adopted in other studies that have looked at concentration dependence (Twyman and Macdonald, 1991; Fucile et al., 1999).

It is not unexpected that the time constants for "within activation" shut times do not depend strongly on concentration at low agonist concentrations, even if the underlying shut states have different numbers of ligands bound. This is because at low concentrations, all association rates have to be relatively slow. For instance, at 0.1 μM the association rate will be at most 10 s^{-1}, even if we assume that the association rate constants have very high values, close to the limit set by diffusion. Such slow rates will have little effect on the eigenvalues of $\boldsymbol{Q}$ (or its subsections) because they are likely to be overwhelmed by other rates out of each state (other elements on the same row of $\boldsymbol{Q}$). The exception to this is obviously the resting state, the only way out of which is association of an agonist, but the concentration dependence of this will affect mainly the "between activation" time constant(s).

It is also possible that some of the short-lived shut states represent a closed state that is distal to open states of the receptor. There could be, for example, a short-lived desensitized state in which the channel enters after activation.

Interpretation of Bursts

The distributions of burst lengths were fitted with four exponential components for the experiments with 0.3 and 1 μM glycine, whereas a fifth component with longer time constant (~50 ms) was necessary to fit adequately the data obtained at 10 μM glycine. The number of components in the burst length distribution should be equal to the sum of the number of open states and the number of short-lived shut states (i.e., those that are deemed to be within the burst; Colquhoun and Hawkes, 1982). In our case, there are at least four open states and three "within-burst" shut states. However only four or five, rather than seven, components were detected in the burst length distribution. This is not surprising, since it is common for components to have time constants that are too similar for them to be separated, or to have areas that are too small to detect.

Burst length distributions showed a concentration dependence analogous to that shown by open period durations. The time constants of the burst length distribution did not change detectably with concentration in the (low) concentration range tested, but shorter bursts were more frequent at the lower concentrations; thus, the areas associated with slower time constants increased with concentration while the areas of the faster components decreased.

The form of the probability density function for burst length distributions (see Colquhoun and Hawkes, 1982, 1995) is similar to that for open times, as it is a function of an initial vector of entry probabilities (the probabilities that the first opening in a burst starts in each of the open states) and a submatrix of $\boldsymbol{Q}$, denoted $\boldsymbol{Q}_{EE}$ (where E denotes the set of open plus short-lived shut states). Agonist concentration will affect the initial vector, and hence the areas of the various components, if the openings that constitute the burst have different levels of ligation for each component. Burst length time constants are determined by the eigenvalues of $-\boldsymbol{Q}_{EE}$: in principle these may change with concentration, but are expected to be almost constant over the low concentration range used here. For the time constants to change significantly, it is the eigenvalues of $\boldsymbol{Q}_{EE}$ that have to change: this will depend on how large the rates of these connections (association rate constant times concentration) are when compared with gating and dissociation rates.

The concentration dependence observed for open periods indicates that when a low concentration of agonist is present, the channel is more likely to visit open states whose lifetime is very short. It is also noteworthy that the time constants of the first two components for the open period and burst length distributions have very similar values (40 μs and 0.4 ms for both distributions), thus suggesting that they originate from single sojourns in the same states of the channel. Indeed, at 0.3 and 1 μM glycine, 70–80% of the bursts occur as single openings, while only ~50% of the bursts at 10 μM glycine are made up of a single opening. The suggestion that the openings in such single opening bursts are very short was confirmed by the inspection of the distribution of open periods per burst restricted to bursts with a fixed number of openings (k). When k = 1, there is an excess of short openings (although some longer openings still occur). As k is increased, the proportion of short open times decreases. This observation shows that bursts of single openings contain openings shorter than average, whereas most of the bursts with several openings are made up of open periods with longer time constants. It is thus reasonable to infer that long bursts (or bursts with several openings) represent oscillations between a set of open and shut states that

Published April 29, 2002

are mostly different from those that are visited during short bursts. Furthermore, the fact that short bursts are more frequent at low concentrations suggests that the short-lived open states contained in such bursts correspond to low liganded states of the receptor. In fact, increasing the concentration of agonist increases the probability of binding more molecules and thus increases the chances of high ligation states (whether they are open or closed) to be occupied.

The Analysis of Correlations

The analysis of correlations is potentially informative about the connectivity between states and in this context was used, for instance, by Fredkin et al. (1985), Colquhoun and Sakmann (1985), and Blatz and Magleby (1989). In our data strong correlations could be demonstrated between the lengths of adjacent open and shut periods and between the lengths of consecutive open periods at all concentrations.

The most striking of these features was the correlation between open and shut times. Short openings tend to occur adjacent to long shuttings, whereas short shut times are often adjacent to long open periods. This information in itself is not enough to allow us to choose a specific topology for the connections in the activation mechanism for the glycine receptor. However, it supports our view that bursts with many openings consist of several long open times, separated by short gaps, very much like the muscle type of nicotinic receptor (Colquhoun and Sakmann, 1985). This is clearly observed at high concentrations, when longer bursts are more frequent, but also applies to the rare long bursts observed at low concentrations. On the contrary, short bursts (that are often made up of a single apparent open period) are often near to longer shut periods. Referring to the topology illustrated in the scheme of Fig. 11 A, this means that short bursts represent oscillations between short-lived open states (lower-liganded open states, very often with a single visit in the open state) and long-lived shut states (lower-liganded shut states). On the contrary, bursts with several openings can be described by oscillations between long-lived open states (higher-liganded open states) and short-lived shut states (higher-liganded shut states). The observed concentration dependence of the various quantities (number of openings per burst, burst length, open periods) can be explained plausibly by assuming that the open states with more bound glycine molecules have longer lifetime, while their adjacent shut states have short lifetimes. This would imply that the configuration in which more molecules are bound to the receptor favors the open state rendering it more stable compared with the shut state. On the other hand, the receptor can still open with fewer bound molecules of agonist, but in this case it opens to a less stable configuration (i.e., with shorter lifetime).

Glycine Receptor Mechanisms

There is little evidence available to guide us in establishing an activation model for a homomeric ligand-gated channel. Apart from glycine receptors, other homomeric receptors do occur in the nicotinic superfamily, notably the α7 neuronal nicotinic receptor, and $GABA_C$ and 5HT3 receptors, but there is very little information on the parameters that would be of interest in establishing an activation mechanism, such as the number of functional agonist sites, though Palma et al. (1996) estimated that at least three molecules of the antagonist methyllycaconitine can bind to α7/5HT3 chimeric receptors. For glycine receptors, the main models that have been put forward so far (Twyman and Macdonald, 1991; Legendre, 1998) refer to heteromeric receptors (which obviously contain fewer α subunits than homomers and may therefore have a different number of functional agonist binding sites).

Although we need more information (e.g. at higher concentrations and in nonsteady-state conditions) before a complete reaction scheme can be proposed, it was nevertheless of interest to see whether our observations are consistent with the simplest mechanism that can be postulated for a homomeric pentamer, which is shown in Fig. 11 A.

This scheme is in strict analogy with that proposed by Monod et al. (1965) and Karlin (1967) as an extension of the del Castillo and Katz (1957) scheme, and with the mechanism proposed by Twyman and Macdonald (1991) for native (heteromeric) receptors with three putative binding sites. Note that the scheme of Fig. 11 A does not include openings from the unbound state R, for the good reason that no openings were detectable in the absence of glycine. Therefore, openings from the unliganded state must be very rare or very short (or both). We have also omitted desensitized states in Fig. 11 A.

Since dissociation from open states is likely to be slow, the direct connections between open states were omitted to give the mechanism in Fig. 11 A. It is shown in the appendix that a scheme of this sort can fit the observations described here, though the fit is unlikely to be unique. According to this fit, channels can open with any number of glycine molecules from one to five bound to the receptor. There is no need at present to postulate any greater complexity than this obvious scheme.

APPENDIX

The rate constants were fitted by a direct maximum likelihood fit of the scheme in Fig. 11 A to the sequence of open and shut times, with exact allowance for missed events, using the HJCFIT program (Colquhoun et al., 1996). A fuller description of this method, and its application to nicotinic receptors is in preparation (unpublished data). The program, and a more

Published April 29, 2002

detailed description in its manual, is available from http://www.ucl.ac.uk/pharmacology/dc.html. The exact missed event correction (Hawkes et al., 1990, 1992) allows calculation of distributions of the events that are actually seen in the presence of limited time resolution (referred to above as "apparent open times"). These distributions will be referred to as HJC distributions.

Nine experiments (three for each concentration) were fitted separately to obtain a set of rate constants that maximized the probability of obtaining the particular sequence of open and shut states observed in each experiment. Fig. 11 shows an example of such a maximum likelihood fit for an experiment performed with 10 μM glycine. The histogram of the observed open periods is shown in Fig. 11 B: the continuous line was not obtained by fitting the histogram, but it is the HJC open time distribution calculated from the fitted rate constants at the resolution imposed in this experiment (30 μs). The dashed line is the open period distribution that would be observed if we had perfect resolution (i.e., if no events were missed). Ideally, all openings would come from the same channel so the entire sequence could be fitted. At the low agonist concentrations used here we cannot be sure of this, so openings were divided into separate bursts (i.e., activations) using the t_{crit} determined in each experiment from the distribution of all shut times. The likelihood of the sequence of events within each burst was separately determined and the rate constants were varied to maximize the product of all the separate likelihoods. The initial and final vectors for each likelihood calculation were calculated as described by Colquhoun et al. (1996, eqs. 5.8 and 5.11). As a consequence of this procedure, shut time distributions (Fig. 11 C) were fitted from the resolution limit only up to the t_{crit} (3 ms for this experiment), since all the shut times that are longer than t_{crit} represent intervals between the activations of different channels and cannot easily be interpreted in terms of the mechanism rate constants. As in Fig. 11 B, the continuous line is the HJC shut time distribution (calculated from the fitted rate constants) and the dashed line is the ideal distribution at zero resolution.

A major advantage of fitting the sequence of openings and shuttings in this way is that it fully takes into account the order in which events occur, i.e., it uses information from the correlation between open times and shut times. Such correlations were described above (Fig. 8). To show that the scheme, and the values for the rate constants, do indeed describe the correlations in the data, conditional distributions like those in Fig. 8 are shown here in Fig. 11, D and E, for open periods adjacent to short (less than 3 ms) and long (>3 ms) shut times, respectively. In each of the plots the continuous line was not fitted to the histogram, but is the conditional HJC distribution calculated from the fitted rate constants. To allow a clearer comparison, the distribution of open periods adjacent to long (short) shut states is scaled and superimposed to the open periods adjacent to short (long) shut states (dashed lines in Fig. 11, D and E). The comparison between D and E shows that the observed correlation between open and shut times was predicted by the proposed model with the fitted rate constants.

Fig. 11 F shows the average of the fitted rate constants for all the nine experiments included in this analysis. Due to the uncertainty in the number of channels in each patch, it was impossible to obtain any information about the rate of entry from the set of long-lived shut states (C) to the set of burst states (E; see Colquhoun and Hawkes, 1982). In the simple model of Fig. 11 A, the only rate constant that determines entry into a burst is k_{+1}. Thus, we arbitrarily decided to fix the first binding rate constant to a value of $k_{+1} = 0.5 \times 10^8\ M^{-1}s^{-1}$, which is plausible in physical terms and comparable to values reported for other ligand-gated channels (e.g., Colquhoun and Sakmann, 1985). An inspection of the fitted rate constants shows that their values are surprisingly consistent from one patch to the other. The agonist effi-

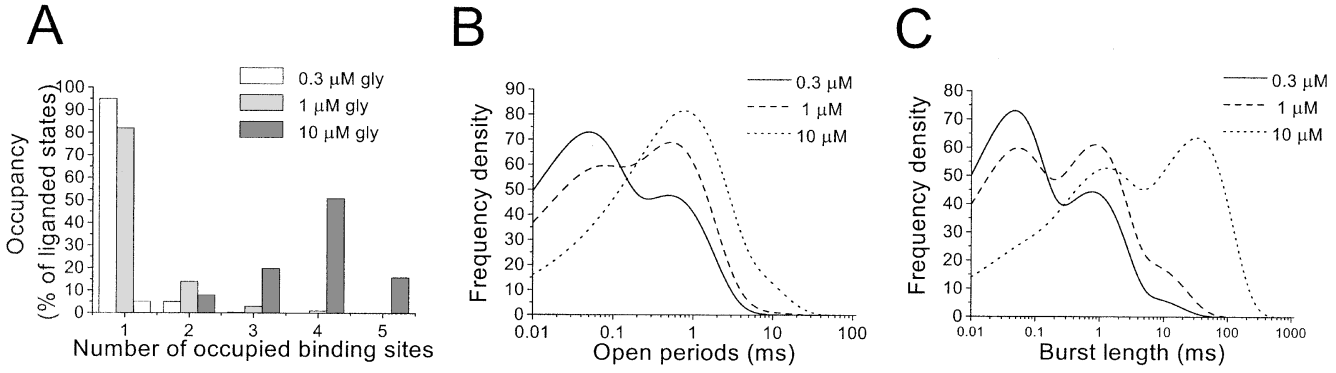

FIGURE 12. The predictions of the fitted model agree with the observed concentration dependence. A shows the equilibrium occupancy (normalized for visibility) of each state of ligation at the different concentrations tested. For singly liganded molecules, for example, the occupancy of AR + AR* are divided by $1 - p_R$, where by p_R is the occupancy of the resting state, R. B shows the concentration dependence of open times as predicted by the fit (c.f. observed distribution in Fig. 3 D). C shows the predicted burst length distributions at the glycine concentrations tested and should be compared with Fig. 6 C. All calculations are based on the average rate constants as in Fig. 11 F.

Published April 29, 2002

cacy (i.e., $E = \beta/\alpha$) for each binding step increases in parallel with the number of agonist molecules bound (Fig. 11 F, last column). This is in agreement with data from the muscle nicotinic receptor in which the efficacy is much higher when two agonist molecules are bound and seems to be a common feature of ligand-gated channels with more than one binding site. However, E does not change by a constant factor with each additional ligand, as assumed by the Monod et al. (1965) mechanism. The predicted true lifetimes of the open states (i.e., the inverse of α) increase as more binding sites are occupied, as also happens for nicotinic receptors (Colquhoun and Sakmann, 1981, 1985; unpublished data). This suggests that the lengthening of apparent open times at higher agonist concentrations seen in our results was not an artifact of missed brief shuttings, but is genuine. No constraints have been imposed on the binding and dissociation rate constants (apart from fixing the first binding rate). Under these conditions, the best fit shows that there is positive cooperativity for the first three binding steps, while some negative cooperativity was needed in the following binding steps, as suggested also for the nicotinic receptor (Jackson, 1988; Sine et al., 1990). Once again, there is not a constant ratio as postulated by Monod et al. (1965) (as found also for nicotinic receptors; unpublished data). Such "mixed cooperativity" has been seen by others too (Jackson, 1989).

Despite the fairly consistent results of the fits, it must be stressed that such results up to now should be considered merely as a proof of existence of at least one set of rate constants that can describe the data for the simplest plausible activation mechanism. It is unlikely that our data contain enough information to determine unambiguously 19 independent parameters. Nonetheless, the relatively small variation of the estimates for each rate constant between different patches and concentrations is an encouraging start, and work (in progress) over a larger concentration range will provide a further test of the simple scheme. For example, it will allow a better test of the possible existence of further, fully occupied distal closed and open states (such as the "reluctant" state proposed by Legendre [1998]).

Using the average rate constants shown in Fig. 11 F, we calculated the equilibrium occupancy of each of the states in the model. The plot of Fig. 12 A shows the occupancy of each level of ligation (open or closed) for the three concentrations tested. At the lowest concentration most bound receptors are monoliganded and very few were more than diliganded. Even at the highest concentration tested, the fraction of fully-liganded receptors is still quite low.

The concentration-dependence of the distributions of the durations of open times and of bursts are plotted in Fig. 12, B and C. These are calculated from the average fitted rate constants, and so are corrected for missed events. Nonetheless, they are remarkably similar to those obtained by directly fitting the distributions of apparent durations with sums of exponentials (Figs. 3 D and 6 C, respectively). The only discrepancy is that in the case of burst lengths, the fitted rate constants predict more numerous long (~100 ms) bursts than were actually observed.

The set of average fitted rate constants in Fig. 11 F gave a Hill slope of 3.5 and an EC_{50} of 10 μM. While the Hill slope is in good agreement with the one measured from the whole cell dose response curves ($n_H = 3.3 \pm 0.2$), the EC_{50} is significantly lower than the observed one (range from 30 to 120 μM, average 78.8 ± 7.2 μM).

This work was supported by the Medical Research Council and the Wellcome Trust (grant 055524).

Submitted: 13 November 2001
Revised: 21 March 2002
Accepted: 4 April 2002

REFERENCES

Akagi, H., K. Hirai, and F. Hishinuma. 1991. Functional properties of strychnine-sensitive glycine receptors expressed in *Xenopus* oocytes injected with a single mRNA. *Neurosci. Res.* 11:28–40.

Blatz, A.L., and K.L. Magleby. 1986. Quantitative description of three modes of activity of fast chloride channels from rat skeletal muscle. *J. Physiol.* 378:141–174.

Blatz, A.L., and K.L. Magleby. 1989. Adjacent interval analysis distinguishes among gating mechanisms for the fast chloride channel from rat skeletal muscle. *J. Physiol.* 410:561–585.

Bormann, J., O.P. Hamill, and B. Sakmann. 1987. Mechanism of anion permeation through channels gated by glycine and γ-aminobutyric acid in mouse cultured spinal neurones. *J. Physiol.* 385:243–286.

Bormann, J., N. Rundström, H. Betz, and D. Langosch. 1993. Residues within transmembrane segment M2 determine chloride conductance of glycine receptor homo- and hetero-oligomers. *EMBO J.* 12:3729–3737.

Colquhoun, D., and A.G. Hawkes. 1982. On the stochastic properties of bursts of single ion channel openings and of clusters of bursts. *Philos. Trans. R. Soc. Lond. B Biol. Sci.* 300:1–59.

Colquhoun, D., and A.G. Hawkes. 1987. A note on correlations in single ion channel records. *Proc. R. Soc. Lond. B Biol. Sci.* 230:15–52.

Colquhoun, D., and A.G. Hawkes. 1995. The principles of the stochastic interpretation of ion-channel mechanisms. *In* Single Channel Recording. B. Sakmann and E. Neher, editors. Plenum Press, New York. 397–482.

Colquhoun, D., A.G. Hawkes, A. Merlushkin, and B. Edmonds. 1997. Properties of single ion channel currents elicited by a pulse of agonist concentration or voltage. *Phil. Trans. R. Soc. Lond. A.* 355:1–44.

Colquhoun, D., A.G. Hawkes, and K. Srodzinski. 1996. Joint distributions of apparent open and shut times of single-ion channels and maximum likelihood fitting of mechanisms. *Phil. Trans. R. Soc. Lond. A.* 354:2555–2590.

Colquhoun, D., and B. Sakmann. 1981. Fluctuations in the microsecond time range of the current through single acetylcholine receptor ion channels. *Nature.* 294:464–466.

Colquhoun, D., and B. Sakmann. 1985. Fast events in single-channel currents activated by acetylcholine and its analogues at the frog muscle end-plate. *J. Physiol.* 369:501–557.

Colquhoun, D., and F.J. Sigworth. 1995. Fitting and statistical analysis of single-channel records. *In* Single-Channel Recording. B. Sakmann and E. Neher, editors. Plenum Press, New York. 483–587.

David, F.N., and D.E. Barton. 1962. Combinatorial Chance. Charles Griffin, London. 356 pp.

Published April 29, 2002

del Castillo, J., and B. Katz. 1957. Interaction at end-plate receptors between different choline derivatives. *Proc. Roy. Soc. Lond. B.* 146: 369–381.

Edmonds, B., A.J. Gibb, and D. Colquhoun. 1995. Mechanisms of activation of muscle nicotinic acetylcholine receptors, and the time course of endplate currents. *Annu. Rev. Physiol.* 57:469–493.

Fredkin, D.R., M. Montal, and J.A. Rice. 1985. Identification of aggregated Markovian models: application to the nicotinic acetylcholine receptor. *In* Procedures of the Berkeley Conference in Honor of Jerzy Neyman and Jack Kiefer. L.M. Le Cam and R.A. Olshen, editors. Wadsworth Press, Monterey. 269–289.

Fucile, S., D. de Saint Jan, B. David-Watine, H. Korn, and P. Bregestovski. 1999. Comparison of glycine and GABA actions on the zebrafish homomeric glycine receptor. *J. Physiol.* 517:369–383.

Gibb, A.J., and D. Colquhoun. 1992. Activation of NMDA receptors by L-glutamate in cells dissociated from adult rat hippocampus. *J. Physiol.* 456:143–179.

Groot-Kormelink, P.J., M. Beato, C. Finotti, R.J. Harvey, and L.G. Sivilotti. 2002. Achieving optimal expression for single channel recording: a plasmid ratio approach to the expression of α1 glycine receptors in HEK293 cells. *J. Neurosci. Methods.* 113:207–214.

Groot-Kormelink, P.J., and W.H.M.L. Luyten. 1997. Cloning and sequence of full-length cDNAs encoding the human neuronal nicotinic acetylcholine receptor (nAChR) subunits β3 and β4 and expression of seven nAChR subunits in the human neuroblastoma cell line SH-SY5Y and/or IMR-32. *FEBS Lett.* 400:309–314.

Hawkes, A.G., A. Jalali, and D. Colquhoun. 1990. The distributions of the apparent open times and shut times in a single channel record when brief events cannot be detected. *Philos. Trans. R. Soc. Lond. B. Biol. Sci.* 332:511–538.

Hawkes, A.G., A. Jalali, and D. Colquhoun. 1992. Asymptotic distribution of apparent open times and shut times in a single channel record allowing for the omission of brief events. *Philos. Trans. R. Soc. Lond. B. Biol. Sci.* 337:383–404.

Jackson, M.B., B.S. Wong, C.E. Morris, H. Lecar, and C.N. Christian. 1983. Successive openings of the same acetylcholine receptor channel are correlated in open time. *Biophys. J.* 42:109–114.

Jackson, M.B. 1988. Dependence of acetylcholine receptor channel kinetics on agonist concentration in cultured mouse muscle fibres. *J. Physiol.* 397:555–583.

Jackson, M.B. 1989. Perfection of a synaptic receptor: kinetics and energetics of the acetylcholine receptor. *Proc. Natl. Acad. Sci. USA.* 86:1–6.

Karlin, A. 1967. On the application of 'a plausible model' of allosteric proteins to the receptor for acetylcholine. *J. Theor. Biol.* 16:306–320.

Keramidas, A., A.J. Moorhouse, C.R. French, P.R. Schofield, and P.H. Barry. 2000. M2 pore mutations convert the glycine receptor channel from being anion- to cation-selective. *Biophys. J.* 78:247–259.

Kins, S., H. Betz, and J. Kirsch. 2000. Collybistin, a newly identified brain-specific GEF, induces submembrane clustering of gephyrin. *Nat. Neurosci.* 3:22–29.

Krishtal, O.A., and V.I. Pidoplichko. 1980. A receptor for protons in the nerve cell membrane. *Neuroscience.* 5:2325–2327.

Kuhse, J., H. Betz, and J. Kirsch. 1995. The inhibitory glycine receptor: architecture, synaptic localization and molecular pathology of a postsynaptic ion-channel complex. *Curr. Opin. Neurobiol.* 5:318–323.

Langosch, D., B. Laube, N. Rundstrom, V. Schmieden, J. Bormann, and H. Betz. 1994. Decreased agonist affinity and chloride conductance of mutant glycine receptors associated with human hereditary hyperekplexia. *EMBO J.* 13:4223–4228.

Laube, B., J. Kuhse, and H. Betz. 2000. Kinetic and mutational analysis of Zn^{2+} modulation of recombinant human inhibitory glycine receptors. *J. Physiol.* 522:215–230.

Legendre, P. 1998. A reluctant gating mode of glycine receptor channels determines the time course of inhibitory miniature synaptic events in zebrafish hindbrain neurons. *J. Neurosci.* 18:2856–2870.

Legendre, P. 2001. The glycinergic inhibitory synapse. *Cell. Mol. Life Sci.* 58:560–593.

Lewis, T.M., L. Sivilotti, D. Colquhoun, R. Schoepfer, and M. Rees. 1998. Properties of human glycine receptors containing the hyperekplexia mutation α1(K276E), expressed in *Xenopus* oocytes. *J. Physiol.* 507:25–40.

McManus, O.B., A.L. Blatz, and K.L. Magleby. 1985. Inverse relationship of the durations of adjacent open and shut intervals for Cl and K channels. *Nature.* 317:625–627.

Monod, J., J. Wyman, and J.-P. Changeux. 1965. On the nature of allosteric transitions: a plausible model. *J. Mol. Biol.* 12:88–118.

Moorhouse, A.J., P. Jacques, P.H. Barry, and P.R. Schofield. 1999. The startle disease mutation Q266H, in the second transmembrane domain of the human glycine receptor, impairs channel gating. *Mol. Pharmacol.* 55:386–395.

Palma, E., S. Bertrand, T. Binzoni, and D. Bertrand. 1996. Neuronal nicotinic α7 receptor expressed in *Xenopus* oocytes presents five putative binding sites for methyllycaconitine. *J. Physiol.* 491:151–161.

Rajendra, S., J.W. Lynch, K.D. Pierce, C.R. French, P.H. Barry, and P.R. Schofield. 1994. Startle disease mutations reduce the agonist sensitivity of the human inhibitory glycine receptor. *J. Biol. Chem.* 269:18739–18742.

Rothberg, B.S., and K.L. Magleby. 2001. Testing for detailed balance (microscopic reversibility) in ion channel gating. *Biophys. J.* 80:3025–3026.

Sambrook, J., and D.W. Russell. 2001. Molecular Cloning. A Laboratory Manual, 3rd edition. Cold Spring Harbor Laboratory Press, Cold Spring Harbor, NY. 1599 pp.

Sigworth, F.J., and S.M. Sine. 1987. Data transformations for improved display and fitting of single-channel dwell time histograms. *Biophys. J.* 52:1047–1054.

Sine, S.M., T. Claudio, and F.J. Sigworth. 1990. Activation of *Torpedo* acetylcholine receptors expressed in mouse fibroblasts. Single channel current kinetics reveal distinct agonist binding affinities. *J. Gen. Physiol.* 96:395–437.

Singer, J.H., and A.J. Berger. 1999. Contribution of single-channel properties to the time course and amplitude variance of quantal glycine currents recorded in rat motoneurons. *J. Neurophysiol.* 81: 1608–1616.

Takahashi, T., A. Momiyama, K. Hirai, F. Hishinuma, and H. Akagi. 1992. Functional correlation of fetal and adult forms of glycine receptors with developmental changes in inhibitory synaptic receptor channels. *Neuron.* 9:1155–1161.

Taleb, O., and H. Betz. 1994. Expression of the human glycine receptor α1 subunit in *Xenopus* oocytes: apparent affinities of agonists increase at high receptor density. *EMBO J.* 13:1318–1324.

Twyman, R.E., and R.L. Macdonald. 1991. Kinetic properties of the glycine receptor main- and sub-conductance states of mouse spinal cord neurones in culture. *J. Physiol.* 435:303–331.

Werman, R., R.A. Davidoff, and M.H. Aprison. 1967. Inhibition of motoneurones by iontophoresis of glycine. *Nature.* 214:681–683.

Wyllie, D.J.A., P. Béhé, and D. Colquhoun. 1998. Single-channel activations and concentration jumps: comparison of recombinant NR1a/NR2A and NR1a/NR2D NMDA receptors. *J. Physiol.* 510:1–18.